Masticatory mechanisms, dental function, and diet in Triassic trilophosaurids (Reptilia: Allokotosauria)

Authors: Mellett, Michael P., Kligman, Ben T., Nesbitt, Sterling J., and Stocker, Michelle R.

Source: Palaeodiversity, 16(1) : 99-124

Published By: Stuttgart State Museum of Natural History

URL: https://doi.org/10.18476/pale.v16.a4

Palaeodiversity 16: 99–124; Stuttgart 29 December 2023. Published online: 18 May 2023, DOI: 10.18476/pale.v16.a4

Masticatory mechanisms, dental function, and diet in Triassic trilophosaurids (Reptilia: Allokotosauria)

Michael P. Mellett, Ben T. Kligman, Sterling J. Nesbitt & Michelle R. Stocker

Abstract

Documenting evidence of feeding behavior in extinct vertebrates is crucial to understanding trophic structure and stability of ecosystems over periods of Earth's history. Direct evidence of trophic interactions in the fossil record is rare, but proxies like dental microwear enable testable hypotheses of feeding behavior in extinct taxa. Here we present new evidence on the masticatory apparatuses and feeding behaviors of Late Triassic (Norian) trilophosaurid reptiles from southwestern North America based on Scanning Electron Microscope (SEM) observation and quantitative analysis of dental microwear in isolated teeth and dentigerous elements. Trilophosaurids are a Late Triassic archosauromorph group known from Europe and North America with distinctive labiolingually expanded teeth that are usually tricuspid; this clade is hypothesized to be herbivorous based on qualitative comparisons of their dentition to those of living taxa. Our study is among the first to infer their diet within a quantitative comparative framework. Analysis of pit-to-scratch ratios (a proxy for the hardness/toughness of dietary intake) indicate dietary disparity between the three examined trilophosaurid taxa, possibly driven by differing plant preferences. Analysis of scratch orientations, caused by contact between opposite teeth during jaw closure (a proxy for the direction of masticatory movements), may suggest derivation of a masticatory mechanism including labiolingual movement in *Trilophosaurus*, differing from the orthal jaw closure mechanism ancestral to archosauromorphs that is likely conserved in the sister group to Trilophosauridae, the Azendohsauridae. Variance in dental microwear patterns between the sampled taxa suggests potential herbivore niche space partitioning amongst North American trilophosaurids during the Norian. Furthermore, microwear evidence for complex masticatory movement in trilophosaurids may suggest previously unknown craniomandibular specializations, highlighting the need for reexamination of trilophosaurid craniomandibular morphology and jaw closure mechanics.

Keywords: Archosauromorpha, *Trilophosaurus*, Chinle Formation, dental microwear, herbivorous reptile, Late Triassic.

1. Introduction

The Triassic Period saw significant compositional and structural changes to ecosystems as life recovered from the Permo-Triassic extinction event (~251 Ma). These include the explosive diversification of archosauromorph reptiles (Ezcurra & Butler 2018), the origin and evolution of dinosaurs (Irmis et al. 2007), and the appearance of other extant tetrapod groups (Padian & Sues 2015). The Triassic radiation of archosauromorphs includes the independent acquisition of dentition inferred to facilitate herbivorous diets in many groups, including rhynchosaurs (e.g., Benton 1984), azendohsaurids (e.g., Flynn et al. 2010; Sengupta et al. 2017; Marsh et al. 2022), trilophosaurids (e.g., Gregory 1945; Robinson 1957; Parks 1969; Demar & Bolt 1981; Spielmann et al. 2008), some aetosauriforms (e.g., Parker 2005; Marsh et al. 2020; Taborda et al. 2021), possibly silesaurids (Nesbitt et al. 2010; Qvarnström et al. 2019), and sauropodomorphs (Mannion et al. 2011). The assumption of herbivorous feeding habits in the aforementioned taxa is largely based on comparison of dental morphology to those of living taxa whose diets can be observed directly; however, this qualitative framework is inherently difficult to test, and it offers little resolution on specific herbivorous dietary preferences (Zanno & Makovicky 2011). Recent advances in quantitative analysis methods assessing diet in Triassic-aged reptiles include large scale morphometric analyses contextualizing jaw and dental shape within a morphospace of living taxa with known diets (i.e., Singh & al. 2021) and Dental Microwear Texture Analysis (DMTA) which uses confocal microscopy to scan tooth surfaces for statistics on their microwear, again in comparison to living taxa with known diets (i.e., Bestwick et al. 2019; Bestwick et al. 2020; Bestwick et al. 2021).

Dietary proxies indicated by quantitative dental microwear analysis act as a parallel line of evidence testing hypotheses posited by morphometric analyses and offer a pathway to improve understanding of Triassic tetrapod dietary function and preferences. Dental microwear includes the pits and scratches formed on a tooth as a result of food-on-tooth and tooth-on-tooth contact, relaying information on both the composition of the diet and the direction of contact, and therefore jaw movement (Ungar 2015). These patterns are the focus of dental microwear analysis, which has variously utilized light microscopy,

Scanning Electron Microscopy, and confocal microscopy to quantify and compare these patterns between species (Simpson 1926; Walker et al. 1978; Zuccotti et al. 1998). Though its use in living and extinct mammals (especially primates) is well established, its application to living and extinct reptiles is burgeoning (Ungar 2015; Bestwick et al. 2019; Winkler et al. 2019). Dental microwear analysis in living lizards (e.g., Winkler et al. 2019), living and extinct crocodylians (e.g., Ősi & Weishampel 2009; Young et al. 2012; Bestwick et al. 2019), extinct lepidosaurs (e.g., Holwerda et al. 2013; Gere et al. 2021), and extinct archosauromorphs (Fiorillo 1998; Williams & al. 2009; Ősi 2011; Mallon & Anderson 2014; Ősi et al. 2014; Varriale 2016; Rivera-Sylva et al. 2019; Kubo et al. 2021) found that microwear patterns are linked to dietary preference and jaw movement in reptiles just as they are in mammals. Only three studies have investigated dental microwear in Triassic-aged tetrapods: Goswami et al. (2005) analyzed dental microwear in the co-occurring cynodont *Dadadon besairiei* and the allokotosaurid *Azendohsaurus madagaskarensis*, finding new evidence for jaw closure mechanics and diets in both taxa. Kubo & Kubo (2014) analyzed dental microwear in six specimens of *Silesaurus opolensis*, finding orthal jaw movement and a likely folivorous diet. Bestwick et al. (2020) sampled dental microwear from a set of pterosaur taxa including the Late Triassic form *Austriadactylus*, finding evidence for an insectivorous diet in that taxon.

To improve understanding of jaw closure mechanics and diets in Triassic reptiles, we chose to sample and analyze dental microwear patterns in trilophosaurid archosauromorphs. Trilophosaurid were medium-sized (<3m) quadrupedal allokotosaurid reptiles (Nesbitt et al. 2015) known from the Late Triassic of North America and Europe, characterized by labiolingually expanded teeth in the maxilla and posterior portion of the dentary, and an edentulous beak-like snout formed by the anterior portion of the dentary and the premaxilla. They represent one of the few abundant medium-sized potentially herbivorous tetrapods in Late Triassic North American ecosystems likely making trilophosaurids a key trophic element in these ecosystems. *Teraterpeton hrynewichorum* (late Carnian, Nova Scotia) represents one of the earliest diverging trilophosaurids, and it bears an edentulous premaxilla and bulbous and somewhat labio-lingually expanded teeth with a single cusp (Sues 2003; Pritchard & Sues 2019). The teeth in the upper and lower jaws of the holotype were found interdigitating (Sues 2003) which indicates that interdigitation may be ancestral for the clade. *Trilophosaurus buettneri* (middle Norian (Adamanian Biozone), southwestern U.S.A), the most abundant trilophosaurid based on reported cranial and postcranial material, bears labiolingually expanded tricuspid dentition (Case 1928a; Case 1928b; Gregory 1945; Parks 1969; Demar & Bolt 1981; Murry 1987; Heckert et al. 2005; Heckert et al. 2006; Mueller & Parker 2006; Spielmann et al. 2007; Spielmann et al. 2008; Kligman et al. 2020a; Chambi-Trowell et al. 2022). Two age classes are thought to be known for *Trilophosaurus buettneri*, an adult/larger class, which has the most material available, and an immature/smaller class only known from one quarry (Otis Chalk Quarry 2; Gregory 1945). Measurements of both the teeth (Parks 1969; Demar & Bolt 1981) and femora (Spielmann et al. 2008) support these age classes, but this picture has been complicated by the cooccurrence of the similarly-sized *Malerisaurus langstoni*, which bears nearly identical femora and is more common than was previously recognized (Nesbitt et al. 2022). *Trilophosaurus dornorum* (middle Norian, Adamanian Biozone, Chinle Formation and Dockum Group) is known from a handful of dentigerous bones (Mueller & Parker 2006) and is characterized by closely spaced, labiolingually expanded, tricuspid dentition with complex cingula. *Trilophosaurus jacobsi* (middle Norian, Adamanian Biozone, Chinle Formation and Dockum Group) is known from fragmentary jaws, isolated teeth, and putative articulated skulls (Murry 1987; Heckert et al. 2006), and it bears tricuspid dentition with complex cingula similar to *Trilophosaurus dornorum*, suggesting synonymy of the taxa (Heckert et al. 2006) or minor interspecific variation (Kligman et al. 2020a). *Trilophosaurus phasmalophos* (middle Norian, Revueltian Biozone, Chinle Formation) is characterized by bicuspid dentition with complex cingulae (Kligman et al. 2020a). The youngest known trilophosaurids, *Variodens inopinatus* and *Tricuspisaurus thomasi* (early Rhaetian, U.K.) bear apicobasally-tall, bulbous, tricuspid dentition (Robinson 1957; Chambi-Trowell et al. 2022). *Spinosuchus caseanus* (von Huene 1932; Spielmann et al. 2008) from the middle Norian of Texas, U.S.A., likely represents postcranial elements of *Trilophosaurus jacobsi* and currently lacks associated dentigerous remains (Nesbitt et al. 2015; Kligman et al. 2020a).

The diet of trilophosaurids has been investigated and speculated on since the first detailed study of its members: Gregory (1945) originally considered *Trilophosaurus buettneri* to be an herbivore that consumed primarily soft vegetation based on the edentulous premaxilla and tooth shape and position. Parks (1969) amended this to potentially include abrasive material (such as quartz grit or phytoliths (Ungar 2015; Strömberg et al. 2016)), and this largely has not been contested by later authors. However, Singh et al. (2021) proposed a notable exception for suggesting a diet of tougher food with limited oral processing or cropping, in contrast to previous suggestions that the beak was specialized for cropping (Gregory 1945; Parks 1969); Singh et al. (2021) also are the only authors who have approached trilophosaurid diet from a quantitative comparative framework. However, the taxon sampling

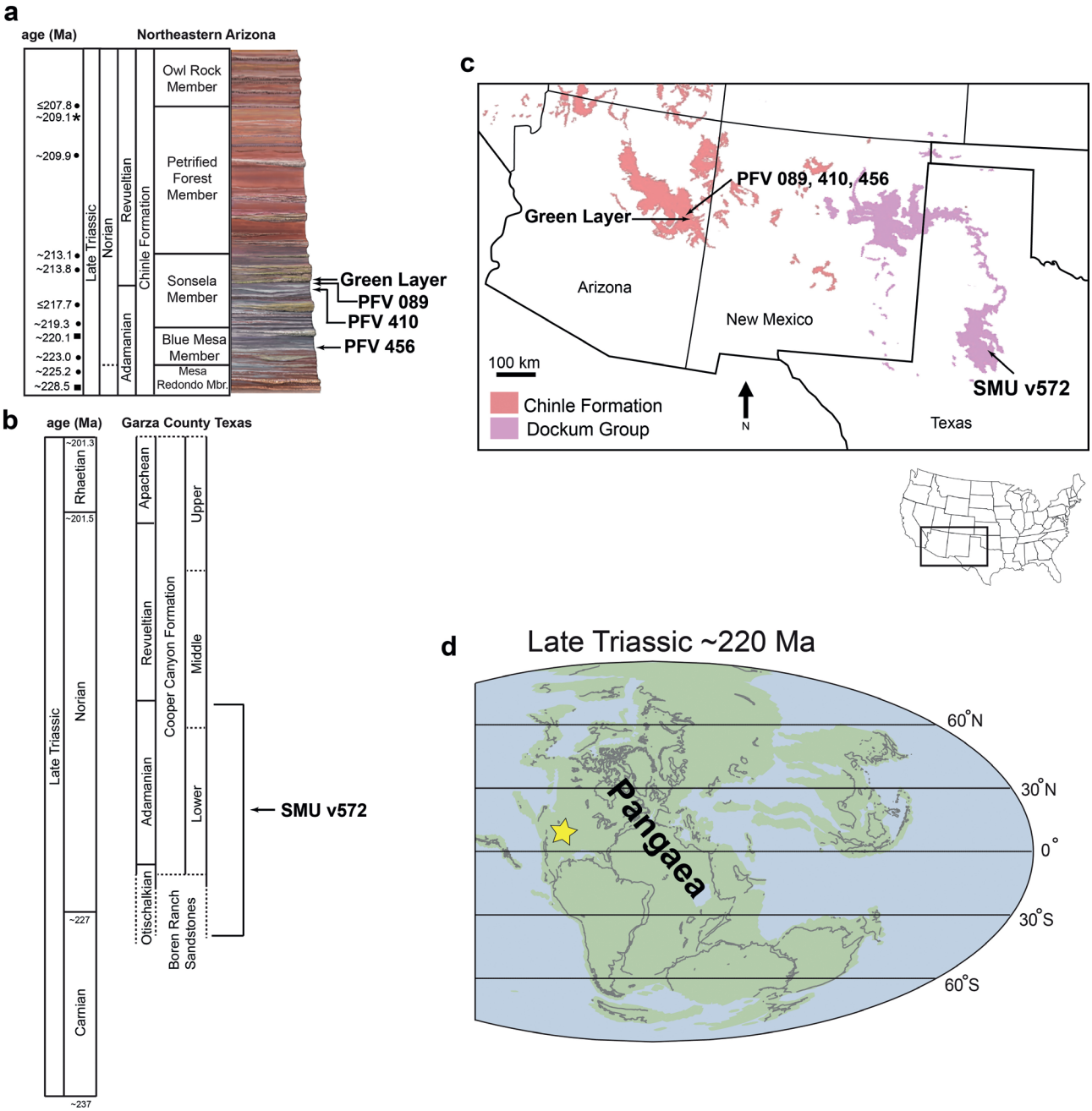

Fig. 1. a: Stratigraphic and geographic context of the Green Layer locality. Stratigraphy and geochronology of the Chinle Formation in northeastern Arizona. U-Pb radioisotopic ages derived from the following: circle = Ramezani et al. (2011), rectangle = Atchley et al. (2014), asterisk = Ramezani et al. (2011); **b:** Stratigraphic and geochronologic context of SMU v572, figure adapted from Lessner et al. (2018). Note that Dockum Group stratigraphy in Scurry County, Texas, lacks current stratigraphic mapping, and the stratigraphy of the Dockum Group in bordering Garza County is used herein; **c:** Present-day geography of Upper Triassic exposures in southwestern U.S.A, and the locations of specimens used in this study; **d:** Paleogeographic map of the Earth at ~ 220 Ma with yellow star marking location of Chinle Formation/Dockum Group deposition.

of Singh et al. (2021) was limited, featuring 2D data from photographs of the lateral side of the dentary of *Trilophosaurus buettneri*. The jaw closure mechanics and diets of trilophosaurids are important for understanding their roles in Late Triassic ecosystems, but this knowledge is limited by a lack of quantitative frameworks for assessing these aspects of trilophosaurid paleobiology.

We approach this knowledge gap through the first dental microwear analyses of trilophosaurid dentition. The aims of the present study include: [1] to provide a quantitative framework for sampling dental microwear patterns in trilophosaurid dentition; [2] to compare microwear data across sampled trilophosaurid specimens and taxa; [3] to reconstruct trilophosaurid jaw closure biomechanics; [4] to infer dietary differences amongst closely related taxa; and [5] to reconstruct the ecological roles and dynamics of trilophosaurid taxa during an interval of floristic and faunistic turnover in the Norian Stage of the Late Triassic.

Institutional abbreviations: DMNH, Perot Museum of Natural History, Dallas, Texas, U.S.A.; PEFO, Petrified Forest National Park, Arizona, U.S.A.; PFV, Petrified Forest Vertebrate (PEFO vertebrate locality number); SMU, Southern Methodist University, Dallas, Texas, U.S.A; UMMP, University of Michigan Museum of Paleontology, Ann Arbor, Michigan, U.S.A.; UWBM, Burke Museum of Natural History and Culture, University of Washington, Seattle, Washington, U.S.A.

2. Geological and paleobiological context

The Upper Triassic sediments of the Chinle Formation and Dockum Group were deposited in a northwest-flowing fluviolacustrine system in western central Pangaea at low paleolatitudes (5°–15°N) from between ~225 to ~205 Ma (Dubiel 1994; Nordt et al. 2015; Rasmussen et al. 2021; Fig. 1). These strata record deposition in a humid equatorial climate prior to ~215 Ma followed by a long term rise in aridity and seasonality beginning at ~215 Ma (Nordt et al. 2015; Lepre & Olsen 2021). A faunistic and floristic turnover, the Adamanian-Revueltian Biozone transition, is concurrent with and possibly linked to that climatic transition (Parker & Martz 2010; Martz & Parker 2017; Baranyi et al. 2018; Lepre & Olsen 2021). This turnover is notable in two tetrapod clades with dentition suggesting herbivorous feeding habits: trilophosaurids (Kligman et al. 2020a) and aetosaurs (Parker & Martz 2010; Martz & Parker 2017).

The paleobotanical assemblage from these strata is represented by macrofossils and microfossil palynomorphs. Over 40 genera are known from the entire Norian age in the Chinle and Dockum basins, including horsetails, ferns, seed ferns, cycads, conifers, gingkoes, and other more obscure and enigmatic herbaceous types (Kustatscher et al. 2018). Conifers are the most diverse group, followed by cycads/Bennettitales, and then ferns (Kustatscher et al. 2018). Horsetails, although low in diversity (five reported species), are abundant and are found in some tetrapod-bearing horizons (Kustatscher et al. 2018; Parker et al. 2021). Other taxa are rare and not diverse (Kustatscher et al. 2018). The microfossil palynomorph assemblage of the Chinle Formation indicates a turnover and reorganization of plant communities concurrent with the Adamanian-Revueltian biozone transition, characterized by a loss of wetland-adapted plants and an increase in xerophytic taxa (Baranyi et al. 2018). Baranyi et al. (2018) hypothesized that this floristic turnover may have driven turnover in tetrapods through reduction of "palatable" (sensu Baranyi et al. 2018) vegetative materials for herbivores.

3. Materials and methods

3.1. Specimen provenance and taxonomy

All specimens described in this study are assigned to Trilophosauridae and, more specifically, within a subclade that includes all other trilophosaurids except *Teraterpeton* based on the presence of the following features as coded by Chambi-Trowell et al. (2022): non-serrated marginal dentition (character 80, state 0); morphology of crown base of the marginal teeth a flattened platform with mesiodistally arranged cusps (character 83, state 2); and tooth shape at crown base of the marginal teeth labiolingually wider than mesiodistally long (character 87, state 2).

Specimen SMU 77695
Fig. 2a–e

Element: Right dentary preserving the distalmost six tooth emplacement sites; the second and fourth tooth crowns are preserved completely (counting from the distalmost position), and the other four tooth emplacement sites show broken tooth bases (Fig. 2c). The apices of the crowns of the second and fourth teeth appear worn. The splenial is present and tightly attached to the medial side of the dentary, covering the splenial facet of the dentary and the Meckelian canal (Fig. 2b).

Taxonomic assignment: *Trilophosaurus buettneri*.

Rationale for identification: SMU 77695 shares the following diagnostic features of *Trilophosaurus buettneri* based on the description of the holotypic material (UMMP 2338) by Heckert et al. (2006): presence of three cusps of subequal height, and labiolingual symmetry of the tooth crown in occlusal view. The recent redescription of the trilophosaurid *Tricuspisaurus thomasi* showed that both these features are also found in the mid-dentary teeth of *Tricuspisaurus thomasi* (Chambi-Trowell et al. 2022), but unlike *Tricuspisaurus*, the dentition of SMU 77695, the holotype, and referred dentary material from *Trilophosaurus buettneri* (UMMP 2338 [Heckert et al. 2006], TMM 31025-5 [Spielmann et al. 2008], TMM 31025-140 [Gregory 1945], etc.) lack a heterodont pattern where the penultimate distal tooth is greatly enlarged relative to adjacent teeth.

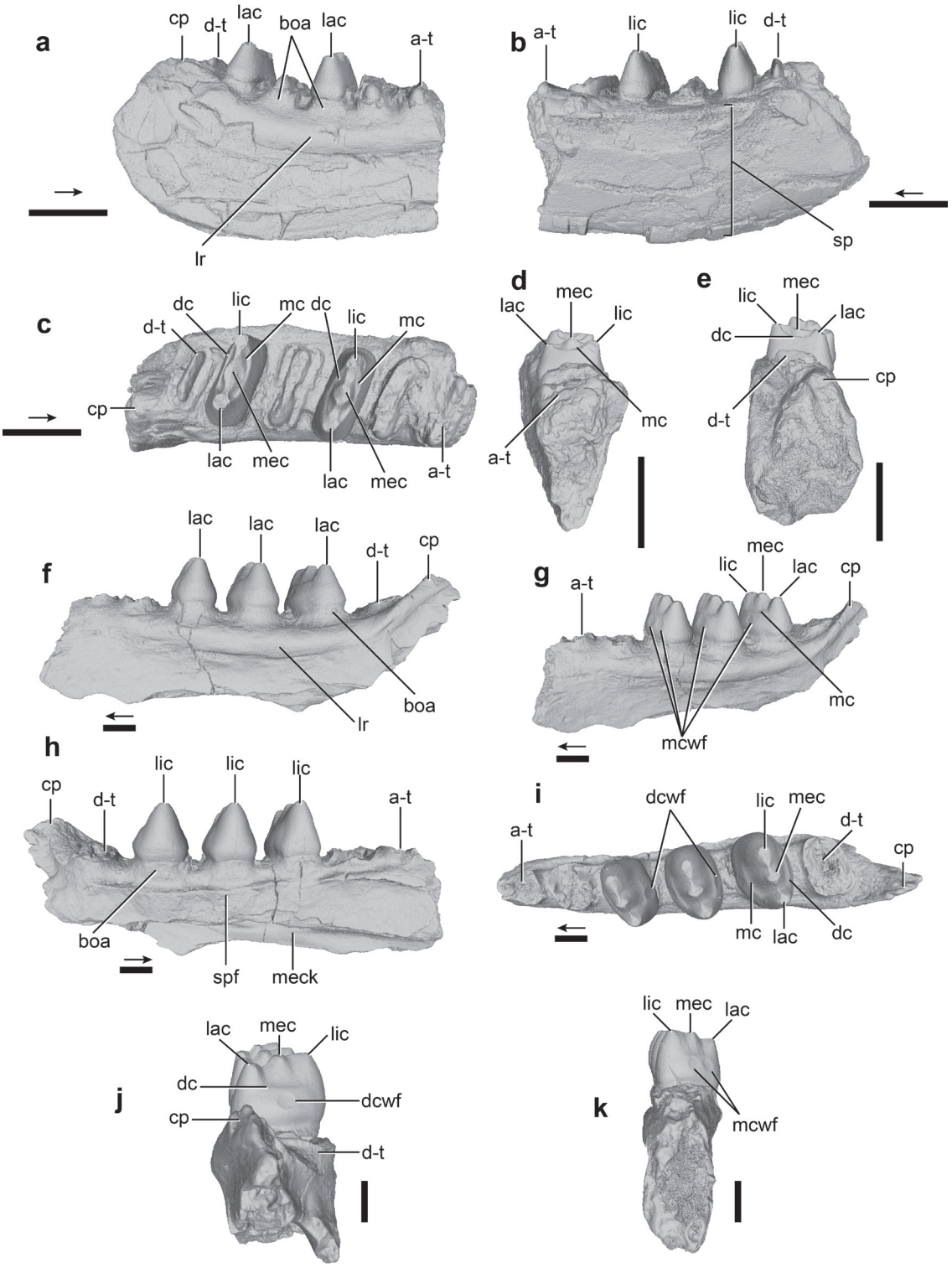

Fig. 2. 3D model images from scan data of SMU 77695 (*Trilophosaurus buettneri* left dentary) and PEFO 43837 (right dentary from the unnamed trilophosaurid morphotype). SMU 77695 in **a:** lateral; **b:** medial; **c:** occlusal; **d:** anterior; and **e:** posterior views. PEFO 43837 in **f:** lateral; **g:** anterolateral; **h:** medial; **i:** occlusal; **j:** posterior; and **k:** anterior views. Abbreviations: a-t, anterior-most tooth; boa, bone of attachment (for teeth); cp, coronoid process; dc, distal cingula; dcwf, distal circular wear facet; d-t, distal-most tooth; lac, labial cusp; lic, lingual cusp; lr, lateral ridge; mc, mesial cingula; mcwf, mesial circular wear facet; mec, medial cusp; meck, Meckelian canal; sp, splenial bone; spf, splenial facet. Arrows point in anterior direction. All scale bars equal 1 mm.

SMU 77695 differs from *Trilophosaurus jacobsi*, *Trilophosaurus dornorum*, and *Trilophosaurus phasmalophos* in the absence of multiple superimposed mesial and distal cingula (Murry 1987; Heckert et al. 2006; Mueller & Parker 2006; Kligman et al. 2020a). SMU 77695 and *Trilophosaurus buettneri* bear dentition with cusps of subequal height, differing from those of the trilophosaurid *Variodens inopinatus* in which the distalmost dentary teeth bear cusps of varying height. Like *Tricuspisaurus* (Chambi-Trowell et al. 2022) and *Trilophosaurus buettneri* (Gregory 1945), the distal-most tooth is relatively smaller than teeth immediately mesial to it.

Stratigraphic placement and associated assemblage: SMU 77695 was collected by Charles McNulty from SMU Locality v572 (Fig. 1b, c), from Dockum Group exposures approximately 10 miles NNW of Colorado City in Scurry County, Texas, U.S.A – near the town of Dunn. Precise stratigraphic and geographic information was not collected; however, this area could be from the Otischalkian or Adamanian Biozones (Parker et al. 2021). In addition to *Trilophosaurus buettneri,* tetrapods with proposed herbivorous feeding habits reported from the Otischalkian and Adamanian Biozones of the Dockum Group in West Texas include the allokotosaurs *Trilophosaurus dornorum* (TTU-P09497, Adamanian biozone) (Martz et al. 2012), *Trilophosaurus jacobsi* (TTU-P09488, Otischalkian biozone) (Mueller 2016), and possibly other trilophosaurids (TTU-P10408, Adamanian biozone) (Mueller 2016), the silesaurid *Technosaurus smalli* (TTU-P09021, Adamanian biozone) (Martz et al. 2012), the aetosaurs *Calyptosuchus wellesi* (TTU-P09420, Adamanian biozone) (Martz et al. 2012), *Typothorax coccinarum* (TTU-P09214, Adamanian biozone) (Martz et al. 2012), *Paratypothorax* sp. (TTU-P09169, Adamanian biozone) (Martz et al. 2012), *Desmatosuchus smalli* (TTU-P09204, Adamanian biozone) (Martz et al. 2012), *Coahomasuchus kahleorum* (NMMNH P-18496, Otischalkian biozone) (Stocker 2013), *Longosuchus meadei* (TMM 31185-97, Otischalkian biozone) (Stocker 2013), *Lucasuchus hunti* (TMM 31100-257, Otischalkian biozone) (Stocker 2013), and other aetosauriforms (TTU P-11750, TTU P-10449, Otischalkian biozone) (Martz 2008), and a kannemeyeriiform dicynodont (TTU-P10402 and TTU-P09417, Otischalkian and Adamanian biozones, respectively) (Martz 2008; Mueller 2016).

Specimen PEFO 43837
Figs. 2f–k, 4e–o

Element: Left dentary fragment bearing three complete tooth crowns and three tooth emplacement sites where broken tooth bases are apparent (Fig. 2i).

Taxonomic assignment: Trilophosauridae, new taxon.

Rationale for identification: PEFO 43837 is a unique, unnamed taxon that shares many features with the holotype right dentary of *Trilophosaurus buettneri* (UMMP 2338; Case 1928a; Case 1928b; Heckert et al. 2006, fig. 3) including labiolingually expanded teeth bearing three apical cusps of subequal height, and like *Trilophosaurus buettneri* it lacks the multiple superimposed mesial and distal cingulae found in *Trilophosaurus jacobsi*, *Trilophosaurus dornorum*, and *Trilophosaurus phasmalophos*. However, unlike in *Trilophosaurus buettneri,* the dentition of PEFO 43837 is mesiodistally more bulbous above/occlusal of the root, more closely resembling the dentition of *Variodens inopinatus* (Chambi-Trowell et al. 2022) and *Teraterpeton hrynewichorum* (Sues 2003, fig. 6); notably, the distal dentition in some specimens of *Trilophosaurus buettneri* (e.g., SMU 77695, TMM 31025-207, TMM 31025-239; Demar & Bolt 1981, fig. 7e, f) are slightly bulbous, but the degree of mesiodistal expansion is less than that of PEFO 43837. Also, unlike *Trilophosaurus buettneri*, PEFO 43837 lacks tooth crown symmetry in occlusal view; instead, the central cusp is connected to the lingual cusp by a straight ridge, and to the labial cusp by a ventrally convex saddle-shaped ridge. It differs further from *Trilophosaurus buettneri* in the presence of flat wear-facets truncating the cusp apices along the same plane. Unlike all other trilophosaurids, PEFO 43837 consistently bears one to two circular wear facets on the mesial and distal surfaces of the distal dentary teeth, an autapomorphic feature suggesting this morphotype may represent a new trilophosaurid species. A full description of this morphotype will be presented elsewhere.

Stratigraphic placement and associated assemblage: Thunderstorm Ridge (PFV 456; Fig. 1a, c) is a conglomeritic horizon bearing unionid bivalve steinkerns, abundant vertebrate coprolites, and micro- and macrovertebrate bones, located in the upper Blue Mesa Member of the Chinle Formation, Adamanian Biozone (Martz & Parker 2017), PEFO, Arizona, U.S.A. See Kligman et al. (2020b) for more detailed description of PFV 456 lithostratigraphy and vertebrate assemblage composition. Allokotosaurids from PFV 456 include the azendohsaurid *Puercosuchus traverorum* (Marsh et al. 2022; PEFO 44767, tooth crown), *Trilophosaurus buettneri* (PEFO 44780, dentary), and the trilophosaurid morphotype represented by PEFO 43837. Other likely herbivorous tetrapods from PFV 456 include the medium-bodied aetosauriforms *Revueltosaurus callenderi* (PEFO 44755) and *Acaenasuchus geoffreyi* (Marsh et al. 2020; PEFO 43699), and the large-bodied aetosaurs *Calyptosuchus wellesi* (PEFO 46222), *Adamanasuchus eisenhardtae* (PEFO 46225), *Tecovasuchus chatterjeei* (PEFO 46468), and *Desmatosuchus spurensis* (PEFO 49568).

Specimen PEFO 42082
Fig. 3j–n (Kligman et al. 2020a, fig. 2)

Element: Isolated tooth.

Taxonomic assignment: *Trilophosaurus phasmalophos* (Kligman et al. 2020a), holotype specimen for the species.

Rationale for identification: See Kligman et al. (2020a).

Stratigraphic placement and associated assemblage: The Bowman site (PFV 089; Fig. 1a, c) is a conglomeritic horizon bearing unionid bivalves and micro- and macrovertebrate bones found in the upper Jim Camp Wash Beds of the Chinle Formation, Revueltian Biozone (Martz & Parker 2017), dated between 218.017 ± 0.088 Ma and 213.870 ± 0.078 Ma (Ramezani et al. 2011), PEFO, Arizona, U.S.A. See Drymala et al. (2021) for a more detailed description and interpretation of PFV 089 lithostratigraphy. The presence of the phytosaur *Machaeroprosopus* (PEFO 34830) at PFV 089 places it just above the Adamanian-Revueltian transition (Kligman et al. 2020a; Drymala et al. 2021). *Trilophosaurus phasmalophos* is the only allokotosaurid known from this locality, and other tetrapods with likely herbivorous feeding

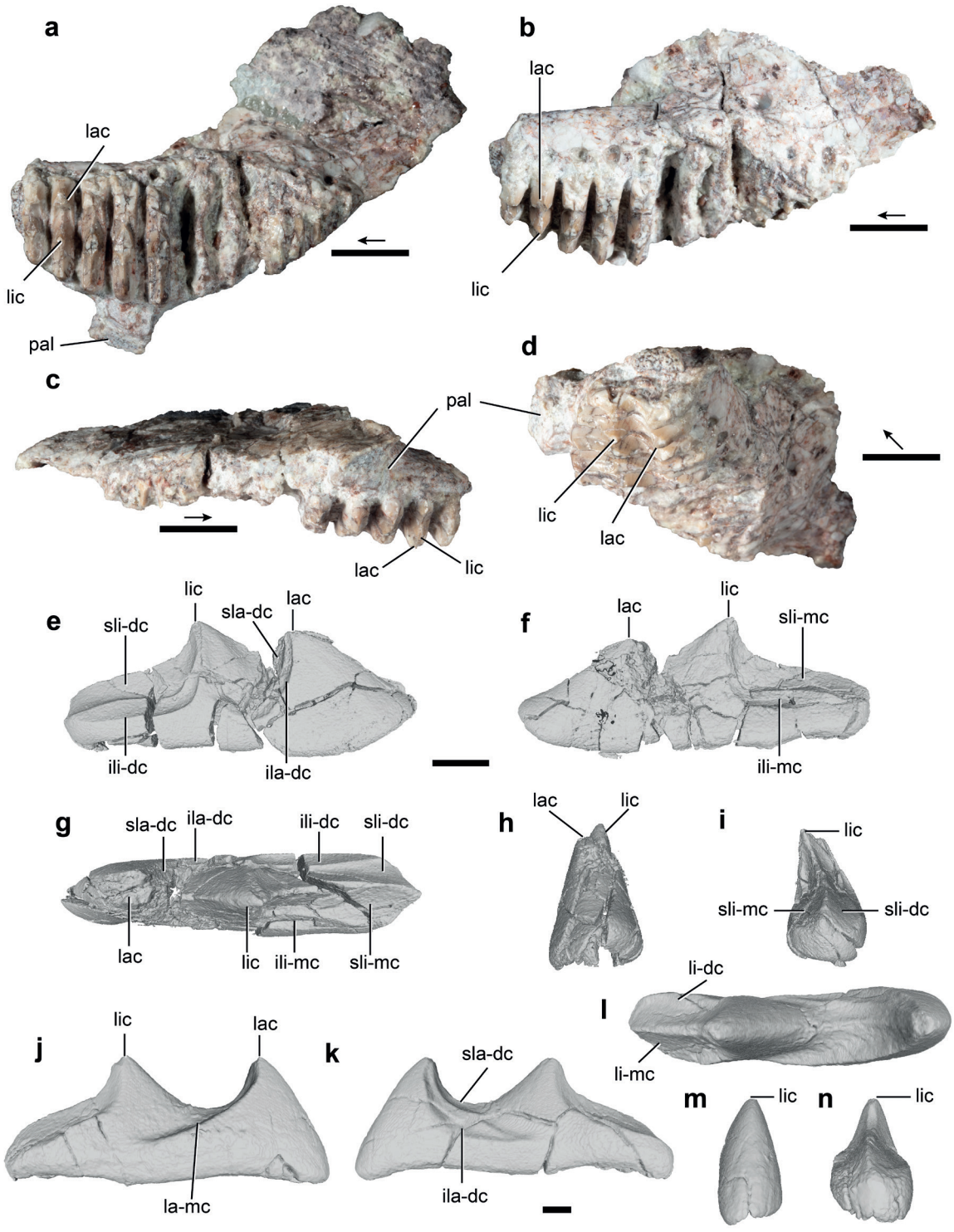

Fig. 3. *Trilophosaurus phasmalophos* dentigerous material and isolated tooth crown. Photographs of UMBW 116791, *Trilophosaurus phasmalophos* maxilla (left) in **a:** ventral; **b:** ventrolateral; **c:** medial; and **d:** anteroventral views. Scale bars equal 5 mm. 3D model images from scan data of DMNH PAL 2018-05-0012 in **e:** ?distal; **f:** ?mesial; **g:** occlusal; **h:** labial; and **i:** lingual views. 3D model images from scan data of PEFO 42082 (the holotype of *Trilophosaurus phasmolophos*) in **j:** ?distal; **k:** ?mesial; **l:** occlusal; **m:** labial; and **n:** lingual views. Scale bar equals 1 mm for **e-n**. Abbreviations: ila-dc, inferior labiodistal cusp; ili-dc, inferior linguodistal cusp; ili-mc, inferior linguomesial cusp; lac, labial cusp; la-mc, labiomesial cusp; lic, lingual cusp; pal, palatine facet of the maxilla; sla-dc, superior labiodistal cusp; sli-dc, superior linguodistal cusp; sli-mc, superior linguomesial cusp; Arrows point in anterior direction.

habits include the medium-bodied aetosauriform *Revueltosaurus callenderi* (PEFO 36759) and a large-bodied paratypothoracine aetosaur (PEFO 34039) (Drymala & al. 2021).

Specimen DMNH PAL 2018-05-0012
Fig. 3e–i (Kligman et al. 2020a, fig. 2)

Element: Isolated tooth.

Taxonomic assignment: *Trilophosaurus phasmalophos* (Kligman et al. 2020a).

Rationale for identification: See Kligman et al. (2020a).

Stratigraphic placement and associated assemblage: The Green Layer Locality (DMNH 2018-05; Fig. 1a, c) is a conglomeritic horizon bearing unionid bivalves and micro- and macrovertebrate bones in the upper Jim Camp Wash Beds of the Chinle Formation, Revueltian Biozone (Martz & Parker 2017), dated between 218.017 ± 0.088 Ma and 213.870 ± 0.078 Ma (Ramezani et al. 2011), located on private land about 20 km east and south of the southern entrance to PEFO. See Stocker et al. (2019) for more detailed descriptions of Green Layer lithostratigraphy and the faunal assemblage. *Trilophosaurus phasmalophos* is the only allokotosaurid recovered from this locality, and other tetrapods with likely herbivorous feeding habits include the medium-bodied aetosauriform *Revueltosaurus callenderi* (DMNH PAL 2018-05-0129), and large-bodied aetosaurs (e.g., DMNH PAL 2018-05-0014).

Specimen UMBW 116791
Fig. 3a–d

Element: Left maxilla with four complete or nearly complete tooth crowns, and other broken teeth.

Taxonomic assignment: *Trilophosaurus phasmalophos*.

Rationale for identification: UMBW 116791 is a left maxilla that is broken at its anterior end, terminating the dentition prior to its natural anterior termination. Crowns of the anterior four teeth are nearly complete and bear the autapomorphic cusp and cingula structure diagnostic of *Trilophosaurus phasmalophos* (Kligman et al. 2020a). Notably, this maxilla confirms the hypothesized labial position of the 'labial cusp' described for isolated teeth of this taxon (Kligman et al. 2020a, fig. 2).

Stratigraphic placement and associated assemblage: The Kaye Quarry (PFV 410, UMBW C2226; Fig. 1a, c), is a conglomeritic horizon bearing unionid bivalves and a mixed micro- and macrovertebrate assemblage in the Jim Camp Wash Beds of the Chinle Formation, dating between 218.017 ± 0.088 Ma and 213.870 ± 0.078 Ma (Ramezani et al. 2011), PEFO, Arizona, U.S.A. (Gonçalves & Sidor 2019). For a more detailed description of the lithostratigraphy of the Kaye Quarry see Gonçalves & Sidor (2019). The Kaye Quarry is located near the Adamanian-Revueltian holochronozone boundary, but its placement above or below this boundary is currently uncertain (Gonçalves & Sidor 2019). Allokotosaurids from the Kaye Quarry include *Trilophosaurus phasmalophos* and an azendohsaurid resembling *Puercosuchus* (UMBW 108383); note that the dentition of *Puercosuchus* lacks morphology associated with herbivory (Marsh et al. 2022). Other likely herbivorous tetrapods from the Kaye Quarry include the medium-bodied aetosauriform *Revueltosaurus callenderi* (UMBW 120018), and large-bodied aetosaurs (UMBW 17294).

3.2. Specimen collection and preparation methods

Collection and preparation methods for PEFO 42082 and DMNH PAL 2018-05-0012 were detailed by Kligman et al. (2020a). PEFO 43837 was collected via screenwashing of fossiliferous sediment at PFV 456 (Thunderstorm Ridge) using the methods described by Kligman et al. (2020a). UMBW 116791 was quarried using hand-tools by the UMBW field team, and subsequently prepared using methods described by Gonçalves & Sidor (2019). TMM 31025-5, TMM 31025-142, and TMM 31025-239 were used for ontogenetic comparison, and were collected by the WPA in the 1930s and 40s; records are on file at TMM. Collection methods are unknown for SMU 77695, but it appears surface collected.

3.3. *Trilophosaurus buettneri* dentary measurements

The labiolingual width, mesiodistal length, and crown height of tooth crowns, as well as the maximum dorsoventral height and labiolingual width of available dentaries were measured using digital (electronic) calipers to the second decimal place. This was done on specimens SMU 77695 (partial mandible), TMM 31025-5 (partial mandible), TMM 31025-142 (partial mandible), and TMM 31025-239 (partial cranium). Other measurements of *Trilophosaurus buettneri* were taken from photographs of isolated teeth as shown by Spielmann et al. (2008) and from photos of TMM 31099-15A #26 (partial mandible). The data are available in Tables 1, 2.

3.4. Digital photography methods

Photographs of specimens PEFO 43837 and DMNH PAL 2018-05-0012 were acquired using a Leica MZ67 stereomicroscope and a Sony NEX-5T digital camera. Image stacking was conducted in Adobe Photoshop CC (https://www.adobe.com/products/photoshop.html). Photographs of UMBW 116791 were acquired using a Nikon ND3400 camera with a macro lens.

3.5. Micro-computed tomographic scan methods

DMNH PAL 2018-05-0012, PEFO 42082, and SMU 77695 were scanned with a Skyscan 1172 Microfocus X-radiographic Scanner at the Virginia Tech Institute for Critical Technology and Applied Science (ICTAS); DMNH PAL 2018-05-0012 was scanned with aluminum and copper filters at a resolution of 11.32 µm, source voltage of 100 kV, and source current of 100 µA. The scanning parameters for PEFO 42082 were detailed by Kligman et al. (2020a). SMU 77695 was scanned with aluminum and copper filters at a resolution of 13.76 µm, source voltage of 100 kV, and source current of 100 µA. PEFO 43837 was scanned with a Nikon XTH 225 ST High-Resolution X-ray

Computed Tomography Scanner in the Shared Materials Instrumentation Facility (SMIF) at Duke University at a resolution of 2.0 μm, source voltage of 225 kV, and source current of 64 μA. CT Scan datasets were processed using Dragonfly 2020.2 (http://www.theobjects.com/dragonfly) to produce 3D mesh reconstructions. Images of 3D surface meshes were produced using Meshlab 2021.07 (https://www.meshlab.net/). Scans of DMNH PAL 2018-05-0012 and SMU 77695 are available online on Morphosource (morphosource.org) under Project ID: 000487183.

3.6. SEM sampling

Teeth were imaged using a Hitachi TM3000 TableTop Scanning Electron Microscope with an accelerating voltage of 15kV. Sites of analysis of PEFO 43837 and PEFO 42082 were taken at a working distance of 5.4–7.5mm, with a magnification of 1200x for PEFO 43837 due to the small areas of enamel visible and a magnification of 600x in PEFO 42082 because larger sections of enamel were available. Sites of analysis of DMNH PAL 2018-05-0012 and SMU 77695 were taken at a working distance of 8.9–14.4mm, and 300x magnification. Pit-to-scratch ratios are expected to be comparable across this range of magnification (Gordon 1988, Mihlbachler & Beatty 2012). Raw images from which sites of analysis were produced are available for DMNH PAL 2018-05-0012, PEFO 42082, PEFO 43837, and SMU 77695 online on Morphosource (morphosource.org) under Project ID: 000487183.

3.7. Sampling organization

Sampling spots were chosen based on presence of visible wear features and the absence of fractured enamel or mineralized layers overcoating the tooth surface (e.g., Figs. 4q, 5a). Spots were further chosen to represent three major heights (apical, middle, and basal) on available sides of the teeth: only one side of DMNH PAL 2018-05-0012 was exposed for analysis (see below), and sites were sampled on the mesial, distal, and lingual sides of the distal-most complete tooth of SMU 77695 in addition to the labial side of the mesial-most complete tooth. Each microwear site analysis was further cropped to a 285 x 216 μm area focused on the area of greatest wear and least debris (following Williams et al. 2009). Sites of analysis were further modified to 44dpi resolution because of an overabundance of apparent features (e.g., >4500 per site analysis) that made measurement at the original resolution impractical.

3.8. Digital measurement procedure

This sampling method (method 1) followed that of Ungar (1995) in that .png sites of analysis were imported into Microware version 4.02 (Ungar 2002), and the major and minor axes of features were selected by mouse clicking. We chose to vary the image contrast and brightness during microwear sampling to better show the total extent of microwear present because, per Gordon (1988), SEM images fail to capture all wear features at a given angle, and any boost to what was captured benefited our accuracy. Data were collected by only M. Mellett to limit inter-observer variation (Grine et al. 2002). Pits were defined as any feature with a length-to-width ratio of less than 4:1, with the rest being scratches (Ungar et al. 1995). Lengths were taken from the same side of a feature if applicable, and widths were taken at the widest point. If a pit immediately followed a scratch, then it was assumed to be two parts of the same feature with only the scratch part counting for the length and width (Gordon 1984). Multidirectional patterns were assumed to be a singular feature if the angle they formed was greater than or equal to 90° and were otherwise measured per section. Features that curved beyond the edge of the site analysis were not counted, but all other partial features were counted to add directionality data at the expense of a slight inaccurate increase in pit count. Recurrent microwear shapes were noted.

3.9. Hand measuring

Two specimens were measured by hand (method 2). PEFO 43837 and PEFO 42082 were sampled exclusively in occlusal view, and sites of analysis were not cropped or downsampled. Features from sites of analysis were measured and marked in Adobe Photoshop version 20.0 following the same cutoffs as above. No directionality data or qualitative patterns were collected for these specimens.

3.10. Analysis procedure

The raw mean and standard deviation scratch orientations provided by the Microware software (method 1) were taken and adjusted for having zero the leftmost value and 180 the rightmost, as well as correction for the angle at which the tooth was placed at in the SEM. Mean angles, standard deviations, and pit-to-scratch ratios were compared where applicable. The use herein of mean directions per site analysis as opposed to directions for all scratches may limit the precision of these results. This means that if an equal number of features were to be directed apically and labiolingually the mean direction would be at a 45º angle. All angles are reported relative to 0º being on the right and 90º directed apically.

We use the standard directional terms for tetrapod teeth as detailed by Smith & Dodson (2003): mesial (= anterior); distal (= posterior); labial (= lateral); and lingual (= medial). Given the mesiodistal symmetry of *Trilophosaurus phasmalophos* teeth, it is as yet impossible to determine the mesial and distal sides of isolated tooth crowns without new material preserving presently unknown portions of the maxillary and dentary dentition. Therefore, we describe isolated *Trilophosaurus phasmalophos* teeth herein as if they were from right dentaries, and place question marks with the use of 'mesial' and 'distal' in reference to direction on the isolated teeth of this taxon (e.g. ?mesial or ?distal).

Microwear analyzed in Microware 4.02 (method 1) presented patterns that were noted and named for their similarity to common shapes and uppercase Latin letters. Scratch patterns where the lines of the symbol correspond to the approximate position of scratches are "A", "C", "H", "L", "S", "U", "V", "Y", "#" and "*" (the last is an asterisk denoting scratches intersecting in a single spot). The last two are a triangle shape, where the scratch starts at a point and expands in width as it expands in length (possibly the same as the artificial scratches described by Gordon (1984)), and sinuous features where the scratch curves back and forth.

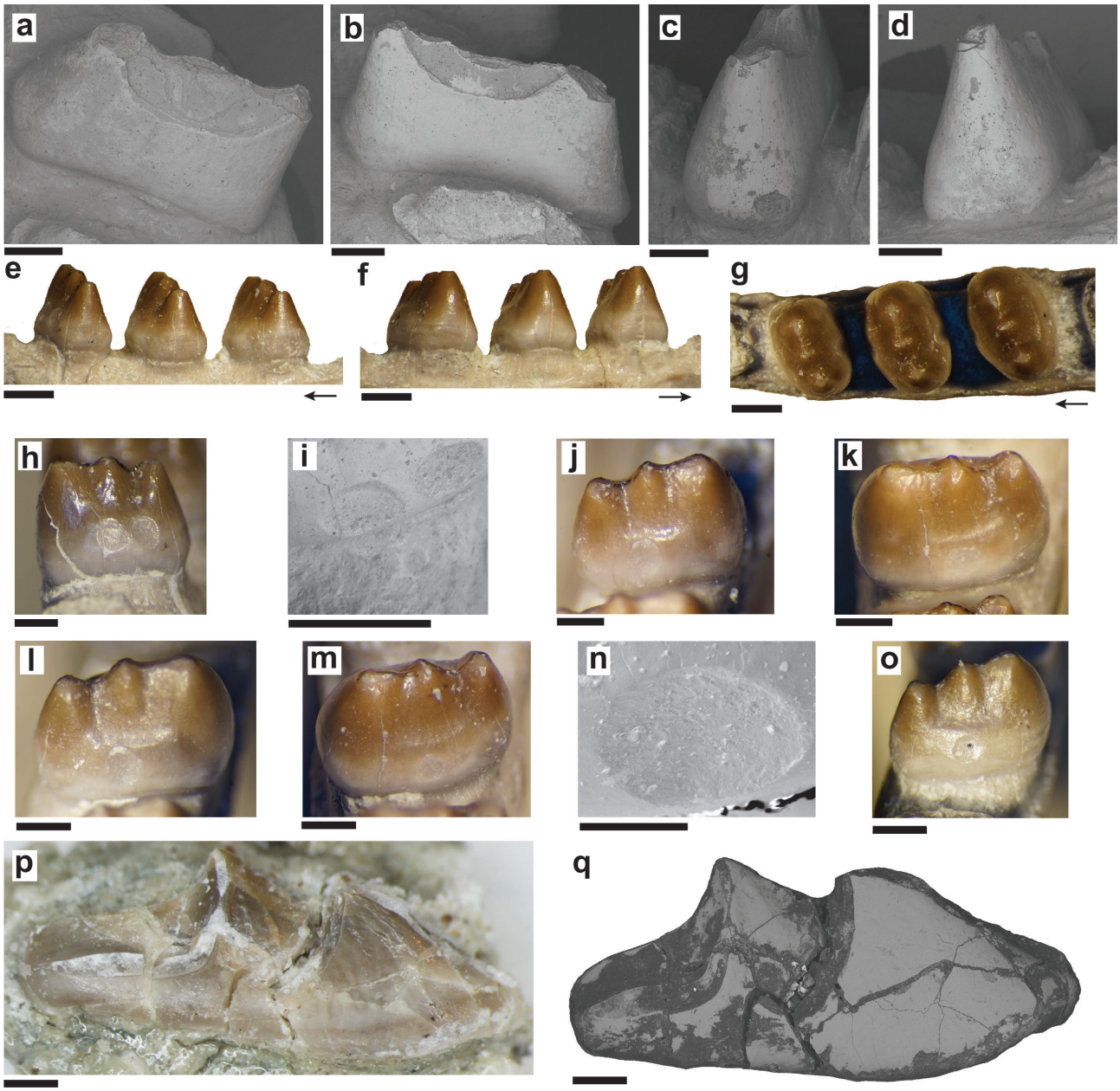

Fig. 4. Photographic and SEM imagery of sampled trilophosaurid tooth crown morphology. SEM images of the distalmost tooth of SMU 77695 (*Trilophosaurus buettneri* left dentary) in **a:** mesial; **b:** distal; and **d:** lingual views. **c:** the labial side of the mesial-most tooth of SMU 77695. **e–h, j–m, o:** photographic and **i, n:** SEM imagery of PEFO 43837 (left dentary from the unnamed trilophosaurid morphotype) including: **h:** mesial-most tooth in mesial; **i:** mesial close-up of circular wear-facets; and **j:** distal views; middle tooth in **k:** mesial and **l:** distal views; distal-most tooth in **m:** mesial; **n:** mesial close-up of circular wear-facet (scale bar equals 300 µm); and **o:** distal views. **p:** hotographic and **q:** SEM imagery of DMNH PAL 2018-05-0012 (*Trilophosaurus phasmolophos* isolated tooth crown). All scale bars equal 1 mm unless otherwise noted. Arrows point in anterior direction.

3.11. Size variation in *Trilophosaurus buettneri* dentition

Holotype and referred dentary material from *Trilophosaurus buettneri* exhibits hypothesized ontogenetic variation in tooth dimensions, tooth replacement patterns, and the presence or absence of cingula (Demar & Bolt 1981).

Gregory (1945) was the first to hypothesize that the smaller sharp-cusped but still laterally expanded teeth found in Otis Chalk Quarry 2 (TMM 31099) belonged to an ontogenetically earlier stage of *Trilophosaurus buettneri*. Parks (1969) provided measurements on the mean widest tooth from "[TMM 31025]-119, -140, -143, -207, -239; [TMM] 31099-18, etc." (p. 4) to support this hypothesis, and Demar & Bolt (1981) included the mean size for all of the teeth in the jaw available from small and large specimens as additional support (from TMM 31025-1, -2, -3, -5, -93–95, -97–112, -115, -116, -119–121, -125, -138, -143, -163, -165, -175, -194, -196, -207, -209, -211, -214, -215, -217, -220–224, -228–230, -233–235, -238, -239, -242, -243, -248–250; TMM 31099-1, -13C, -13D, -13F, -14, -15, -15A, -16–22). However, no rigorous tests of that hypothesis have been conducted on *Trilophosaurus* teeth, and they await analysis with modern methods such as osteohistology and CT scanning. Following the efforts of Parks (1969), we digitally and manually measured aspects of tooth and dentary size to better understand the range of putatively adult tooth and dentary sizes compared to putatively immature ones. We used SMU 77695 and TMM 31099-26 (formerly TMM 31099-15A as it is herein referred to) as immature examples and NMMNH P-34374, P-34373, P-34291, (the specimen from) SMU 252, MNA 7064, TMM 31025-143, 31025-5, 31025-142, and 31025-239 as putative adult examples. Our results mirror the previous studies in finding the mean size of teeth with the proposed 'immature' morphology to be smaller than those of adults. More specifically, we provide measurements showing that the teeth preserved near the back of the jaw (as in SMU 77695) are among the largest in the jaw, so whereas the size of SMU 77695 teeth overlap with the size of isolated teeth and associated teeth from the front of the jaw from 'adults', they are dwarfed by the size of equivalent 'adult' teeth (Tables 1, 2). Curiously, the isolated teeth shown by Spielmann et al. (2008) were all smaller than the average size for the taxon (Table 2). Additionally, the maximum dorsoventral height and labiolingual width of the SMU 77695 dentary is roughly half the size of that for 'adult' specimens (Tables 1, 2). Though we did not explicitly test the hypothesis that the smaller, sharper teeth are from immature *Trilophosaurus* individuals, our results do not reject the idea that SMU 77695 belongs to an immature *Trilophosaurus buettneri*, and we refer to it as such in this paper.

3.12. Preservational effects on SMU 77695

Two sites of analysis on the mesial side of SMU 77695 that were examined for microwear partially overlapped (less than 1/3 of each site analysis), and the resulting mean scratch directions are 87° different from each other. This large discrepancy despite how close the areas are may suggest that debris on the tooth obscured too much wear to determine the original angles of microwear (Fig. 5b). As such, analyses are included with and without the mesial side for this specimen. The distal side has less surface debris so is expected to accurately preserve the microwear signal.

4. Results

4.1. *Trilophosaurus buettneri* measurements comparison

The mean length, width, and height of proposed immature *Trilophosaurus buettneri* teeth were on average 0.67, 0.59, and 0.88 times as large (respectively) as the proposed adult teeth (Tables 1, 2).

4.2. Results by specimen

Specimen SMU 77695

Qualitative features of SMU 77695: The more mesial tooth has greater surface debris on the mesial and distal sides, so only the distal-most tooth was sampled on those sides (which also had more debris on the mesial surface) and one image was taken of the labial side of the mesial tooth. Both teeth lack the sharp cusps of TMM 31099-15 (Demar & Bolt 1981, fig. 6), and the more mesial tooth has rounded edges at the apex of the cusps suggesting this is a wear facet and not a break (the distal tooth appears broken at the cusp). The enamel above the cingula is obscured by surface debris and was not analyzed.

All sites of analysis (="images" per Kubo & Kubo (2014) and "microwear sites" per Goswami et al. (2005)) contained microwear curving in the shape of a 'C', 'U', comma, or 'J' on the distal tooth. All sites of analysis also contained microwear converging as in a 'V', 'A', or sometimes 'L'. Eight of thirteen sites analyzed have microwear converging as a 'H' or like an asterisk, although none are in the form of a hashtag. Eight sites analyzed have the triangle shape as above. Six sites analyzed have sinuous features.

Pit-to-scratch ratios: SMU 77695 was measured using method 1 and had 11,980 wear features across thirteen sites of analysis and parts of two teeth (see Methods for explanation), although surface debris likely obscured some, especially on the mesial side of the distal-most tooth (Table 3). The pit counts are likely inflated due to features ending outside the edge of the sites of analysis and appearing artificially short (Gordon 1988). The pit to scratch ratio was 0.526:1. If the mesial-most tooth is excluded the ratio was 0.540:1, and if both that and the mesial side of the distal-most tooth is excluded (discussed below) the ratio was 0.434:1.

Microwear orientations: The mean microwear orientation of each site had a range of 164° (Table 3). The mean angle was 107.6° with a majority of angles directed towards the central cusp and both labial and lingual wear directed vertically (Fig. 5b–h). Two sites on the mesial side partly overlapped, and the angles differed by 87.0° (Fig. 5b, see Methods for discussion). The mean standard deviation was less consistent than above with a mean of 52.7° but a range of 48.0°. By location, the mesial side of the distal-most tooth had a mean direction of 90.8° and a range of 163.0° with a mean standard deviation of 53.5° and a range of 27.4° (five sites). The labial side of the mesial-most tooth had a mean direction of 106.5° and a range of 9° with a mean standard deviation of 36.7° and a range of 9.341° (two sites). The distal side of the distal-most tooth had a mean direction of 127.8° and a range of 148.0° with a mean standard deviation of 60.2° and a range of 36.0° (five sites). Lastly, the lingual side of the distal-most tooth had a mean angle of 93.0° and a mean standard deviation of 43.5° (one site).

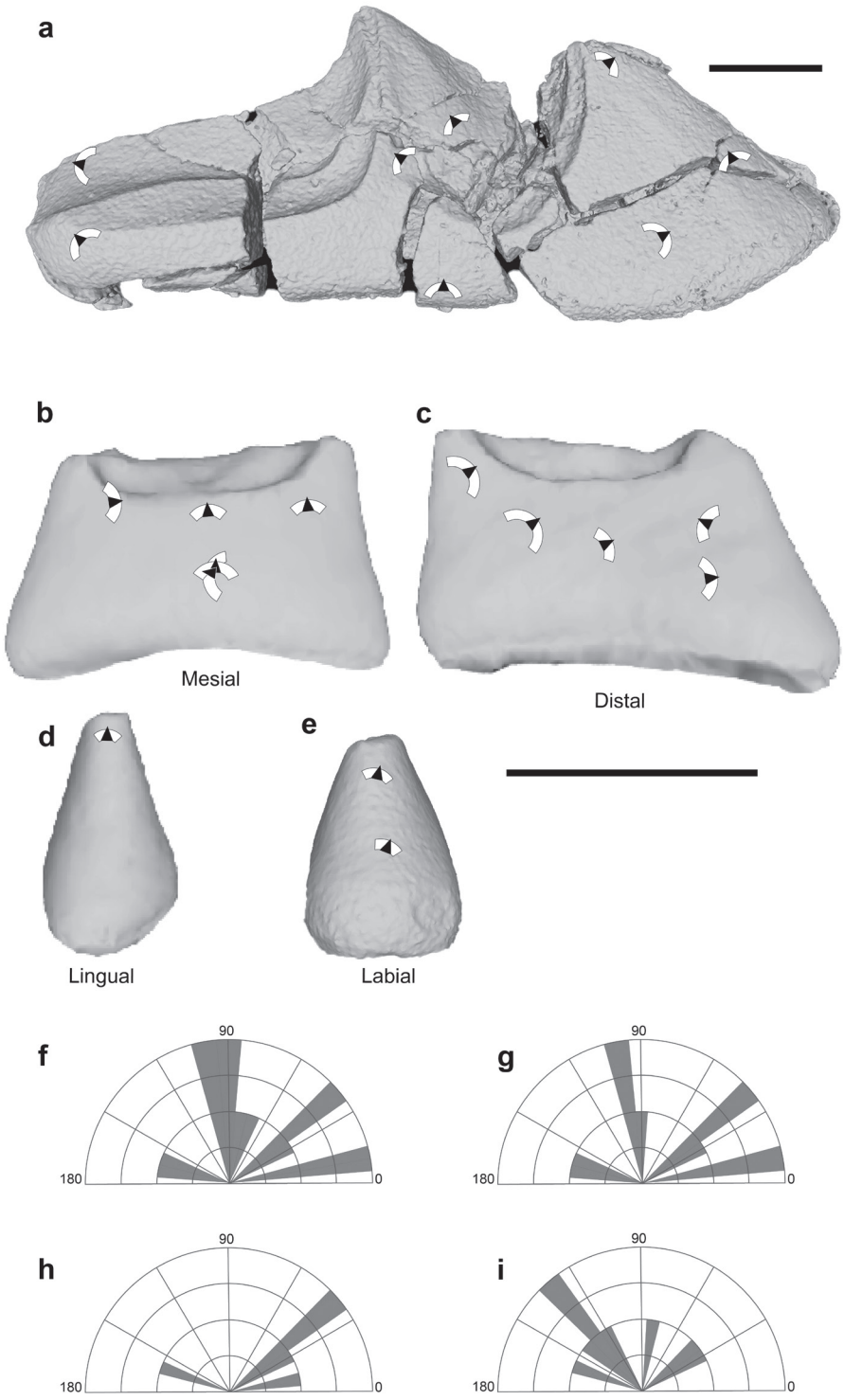

Fig. 5. Whole tooth images of the **a:** ?mesial side of DMNH PAL 2018-05-0012; **b:** the mesial side of the distal-most SMU 77695 tooth; **c:** the distal side of the distal-most SMU 77695 tooth; **d:** the lingual side of the distal-most SMU 77695 tooth; and **e:** the labial side of the mesial-most SMU 77695 tooth demonstrating the distribution of predominant microwear angles. Arrows denote mean direction and arcs denote the standard deviation of the angles. Rose diagrams of **f–h:** SMU 77695 and **i:** DMNH PAL 2018-05-0012 showing the distribution of mean angles. **f** includes angles from all sides of SMU 77695 including data from the mesial-most tooth, **g** only shows the mesial and distal sides of the mesial-most tooth, and **h** only shows the distal side of the mesial-most tooth. All scale bars equal 1 mm.

Specimen PEFO 43837

Qualitative features of PEFO 43837: The most striking aspects of PEFO 43837 are the large circular wear facets occurring on all the preserved teeth, initially reported by Kligman et al. (2020a) and first figured in the present manuscript (Figs. 2g, i, k, 4h–o). Tooth three (distalmost complete tooth, Fig. 4m–o) bears one basal wear facet on the mesial and distal sides each, in addition to the apical wear facets (Figs. 2i, 4l). Basal wear facets are roughly circular concave depressions into the dentine of the tooth, with an internal surface of exposed dentine and rounded edges. Surface debris was found to have accumulated in all wear facets making further description somewhat difficult without additional preparation. The apical wear facets occur at the tip of all three cusps and along the ridge connecting the labial and central cusps. Edges are rounded, and dentine is partially visible underneath the surface debris. Irregular gouges are visible on parts of the enamel. Tooth two (middle complete tooth, Fig. 4k, l) is nearly identical to tooth three, with circular concave basal wear facets and apical wear facets on the cusps and one ridge. The interiors of the basal wear facets are again rough, with more abrupt edges on both sides. The apical wear facets are similar, with little dentine exposed and no obvious gouges. Tooth one (the mesial-most) features one basal wear facet distally and two mesially (Fig. 4h–j). The dentine exposed in the wear facet is rough, and for the double facet the edges are sharpest basally and medially, being more rounded on the apical, labial, and lingual sides (which may be the same as in the other two teeth). The apical wear facets are much the same as tooth one. Because no enamel remains within the wear facets, they were not included in the microwear analysis given the uncertain nature of dentine microwear signals (Tseng 2012). Faint cingula between the first and third cusps are visible on both sides of all teeth.

Pit-to-scratch ratios: PEFO 43837 was measured using method 2 and had a total of 2,476 microwear features across eight sites of analysis and three teeth, although doubtless some features were covered by debris (Table 5). The total pit to scratch ratio of this specimen was 1.836:1 (Tables 5, 7) with a median of 1.771:1.

Specimen PEFO 42082

Qualitative features of PEFO 42082: There is little to no enamel remaining on the ?mesial side of this specimen (bearing two cingula on the labial half). The ?distal side has patches of enamel remaining but large sections are missing. Sites of analysis sampled regions of well-preserved enamel on the ?distal side of the tooth. Other features were described by Kligman et al. (2020a). Little to no surface debris was observed.

Pit to scratch ratios: PEFO 42082 was measured using method 2 and had 2,558 features across four sites of analysis, although doubtless some features were missing because of the incomplete enamel. The pit-to-scratch ratio was 0.448:1 (Table 6).

Specimen DMNH PAL 2018-05-0012

Qualitative features of DMNH PAL 2018-05-001: Micro-computed tomographic scan data revealed features of the ?mesial (see above) side of the tooth which were not described by Kligman et al. (2020a) because matrix obscures the surface. This specimen is crushed, propagating cracks throughout the tooth; however, enamel is well preserved on the ?distal side. The lingual cusp is more complete in this specimen than in PEFO 42082, but the labial cusp is less complete than in PEFO 42082. This specimen also bears other features not found in PEFO 42082, namely double cingula beneath both cusps on the ?distal side. There also appears to be less labiolingual distance between the cusps than in PEFO 42082 with a longer section posterior to the second cusp and a slightly sharper ridge between the first and second cusps. These features are within normal variation for the species as reported by Kligman et al. (2020a). Mineral growth and other surface debris obscure parts of the enamel on the exposed side.

All sites of analysis contained microwear curving like the shape of a ‘C’ or comma, forming a ‘U’, and converging in the shape of a ‘V’, ‘A’, or ‘Y’. Several sites of analysis had points of dense microwear in one spot akin to an asterisk or pound sign. Seven of the eight sites of analysis also had microwear starting at a point and broadening in an isosceles triangle shape (one feature). Five site analyses had features that were sinuous.

Pit-to-scratch ratios: DMNH PAL 2018-05-0012 was measured using method 1 and had 7,495 features across eight sites of analysis, although some debris persisted lowering the total count (Table 4). The number of pits may be inflated from including partial features at the edge of the site analysis that appeared to have the length to width ratio of a pit but may have extended beyond the edge of the image. The pit-to-scratch ratio was 0.404:1.

Microwear orientations: The mean microwear orientation of each site had a range of 136.5°, with adjusted angles both nearly vertical and nearly horizontal (Fig. 5a, 5i). The mean angle was 71.6°; however, the majority of scratches were at least somewhat deflected lingually. This was especially strong on the lingual cingulum, which had an angle of 12.8°, and was only contradicted near the base of the tooth and at the top of the cusp (Fig. 5a). The mean standard deviation was 68.0° with a range of 23.2°.

5. Discussion

5.1. Total feature counts

The total number of features per site that were analyzed was extremely high for method 1 (estimated in one of the sites of analysis to be in excess of 4,500 features based on extrapolating the results of 1/9th of the site analysis analyzed without any downsampling), with even the downsampled sites of analysis having more features than entire jaws of teeth of reptiles and mammals with various diets in other studies (i.e., Gordon 1988; Williams et al. 2009; Kubo & Kubo 2014; Xafis et al. 2020). The cause of this is unknown; taphonomic processes usually result in lower wear counts (King et al. 1999), and counts were universally high for the sites of analysis analyzed in Microware 4.02. Additionally, counts were similar between *Trilophosaurus buettneri* (SMU 77695) and *Trilophosaurus phasmalophos* (PEFO 42082, DMNH PAL 2018-05-

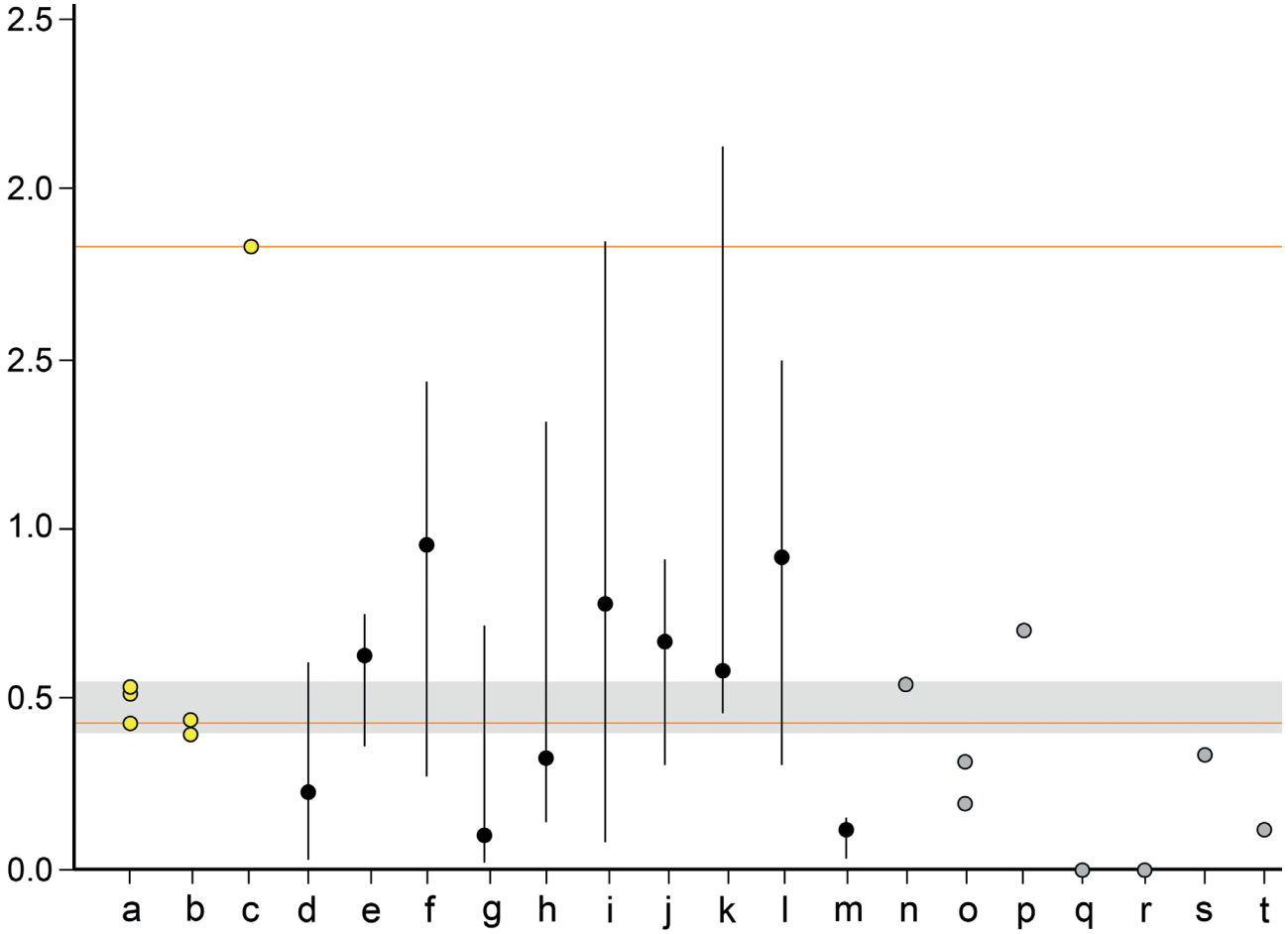

Fig. 6. Graph of pit-to-scratch ratios. Black points indicate mean ratios across taxa, gray points indicate singular taxon ratios (from Pinto Llona (2006) [**o**, **p**]; Holwerda et al. (2013) [**n**]; Kubo & Kubo (2014) [**c**–**m**, **q**–**t**], yellow points indicate ratios of specimens from this study, vertical black lines indicate the range of values across taxa, horizontal orange lines indicate the value of the point they pass through, and the gray horizontal box indicates the range of values found for *Trilophosaurus buettneri* and *Trilophosaurus phasmalophos*. **a:** mean pit-to-scratch ratios for *Trilophosaurus buettneri* with both teeth, distal tooth, and distal side of distal tooth in descending value; **b:** mean ratios for *Trilophosaurus phasmalophos* with PEFO 42082 and DMNH PAL 2018-05-0012 in descending value; **c:** mean ratio for the unnamed taxon (PEFO 43837); **d:** data for grazers; **e:** data for mixed feeders; **f:** data for browsers; **g:** data for folivores (i.e. non-grass foliage); **h:** data for foli-frugivores; **i:** data for frugivores; **j:** data for tuber-feeders; **k:** data for carnivores; **l:** data for insectivores; **m:** data from hadrosaurs; **n:** data from *Carinodens belgicus*; **o:** data from extant (above) and fossil (below) brown bears (*Ursus arctos*); **p:** data from a cave bear (*Ursus spelaeus*); **q:** data from *Diplodocus*; **r:** data from *Azendohsaurus madagaskarensis*; **s:** data from *Camarasaurus*; **t:** data from *Silesaurus opolensis*.

0012) (although slightly higher for the latter) suggesting that this was not strongly impacted by geographic location, life stage, or time of occurrence. It has been suggested that dust and grit in the diet can result in many of the scratches observed on teeth (Ungar 2015), so it is possible that these animals ingested large quantities of these materials. The unnamed taxon (PEFO 43837) exhibited less than 1/3 of the downsampled average feature counts, and the specimen of *Trilophosaurus phasmalophos* also sampled via method 2 (PEFO 42082) exhibited ~2/3 of those average feature counts, but this could be a result of the greater magnification and therefore smaller sampling area (0.0571 mm^2 vs. 0.06156 mm^2) as well as scanning from the occlusal view which did not always have perfectly perpendicular image capture. However, it is worth noting that some research has found making casts of the teeth can significantly remove features (Mihlbachler et al. 2019), implying that other studies may have artificially low counts rather than ours having artificially high counts; we imaged microwear directly from tooth surfaces, not from

casts. Another possibility is that diets in these taxa were extremely high in fiber. While fiber does not directly produce wear (Covert & Kay 1981), it requires significantly more chewing in mammals and allows for a greater likelihood of wear from exogenous grit ingested on or with the food (Kubo & Yamada 2014). The mean feature count per site was higher in both specimens of *Trilophosaurus phasmalophos* (PEFO 42082, DMNH PAL 2018-05-0012) when compared to *Trilophosaurus buettneri* (SMU 77695) and the unnamed taxon (PEFO 43837) for the corresponding counting method (method 1 vs method 2).

5.2. Diet hardness and toughness

Pit-to-scratch ratios have been used to determine broad dietary differences in mammals, with pits being correlated to woody vegetation, bone, mollusk shells, similarly "hard" foods, and sand or gravel (Ungar 1994; Hedberg & DeSantis 2017), and scratches being correlated with phytoliths (silica incorporated into the bodies of plants to discourage grazing) and quartz grit and dust (Ungar 2015) (Fig. 6). *Trilophosaurus phasmalophos* (PEFO 42082, DMNH PAL 2018-05-0012) exhibits proportionally mesiodistally narrower teeth with sharp cusps, features not associated with crushing or grinding, and has a moderately low pit-to-scratch ratio (combined average of 0.425) consistent with a diet lacking in significant gravel, hard seeds, or woody vegetation, but still consuming some hard foods. PEFO 43837 proportionately has the mesiodistally broadest teeth that are bulbous and has the highest pit-to-scratch ratio (mean 1.836, median 1.771) consistent with a diet that may include woody vegetation, hard seeds, or incidental gravel. Surprisingly, the immature *Trilophosaurus buettneri* (SMU 77695) pit-to-scratch ratio (0.526) is like that of *Trilophosaurus phasmalophos* (PEFO 42082, DMNH PAL 2018-05-0012) (0.425) despite its morphological similarity to the unnamed taxon (PEFO 43837) (1.836). Indeed, if mesial-most tooth and the mesial side of the distal-most tooth are discounted for the sampled tooth of SMU 77695, the pit-to-scratch ratio (0.434) overlaps with that of the range of the two specimens of *Trilophosaurus phasmalophos* (0.448 for PEFO 42082 and 0.404 for DMNH PAL 2018-05-0012) (Table 7). This suggests that despite having different tooth shapes and occurring at slightly different times in the geologic record, immature *Trilophosaurus buettneri* and *Trilophosaurus phasmalophos* had a similar dietary hardness and therefore potentially dietary preferences. The sharper cusps and more pronounced cingula of teeth of immature *Trilophosaurus buettneri* compared to those of adults may be related to this similarity of microwear, and potentially indicate a different diet than in adults that possess rounded cusps and less pronounced cingula (Demar & Bolt 1981). The pit-to-scratch ratios we observed in the trilophosaurid taxa are within the ranges also observed in mammalian carnivores (Fig. 6), but even the downsampled feature densities exceed those of sampled mammalian carnivores by two orders of magnitude (and the theoretical maximum densities exceed those of any mammal listed by Kubo & Kubo 2014). Such high densities indicate abrasives were either extremely abundant in diets, or more likely significant oral processing occurred to produce them (Kubo & Kubo 2014; Ungar 2015). It is also worth noting that as *Trilophosaurus buettneri* (and presumably other trilophosaurids) replaced their teeth throughout their life (Demar & Bolt 1981) so any particular tooth could potentially be worn down without negative impacts much faster than in most mammals, which have limited tooth replacement. Given these observations, our data, and evidence from other studies, we do not consider the trilophosaurid taxa sampled herein to be carnivorous but cannot exclude the possibility they were omnivorous.

Parks (1969) reported the presence of wear facets along the ridges of the crown, which he interpreted as evidence of a diet high in dust or other highly abrasive material. More recently Singh et al. (2021) identified *Trilophosaurus buettneri* as a tough food limited oral processor, although what constitutes a tough food has been poorly and rarely quantitatively studied beyond correlation to fiber content (Ungar 2015). Parks suggested that the phytoliths of contemporary horsetails could have produced the wear he observed on some of the ridges of teeth of *Trilophosaurus buettneri*. Others have described cycads and other dense gymnosperms as likely tough food items (Goswami et al. 2005), with ferns being considered soft (Williams et al. 2009) for the plants known from the Chinle Formation and Dockum Group (Kustatscher et al. 2018). It is also important to consider that mammals with the softest diets today have very little microwear at all, whereas tough grazers have many scratches, browsers have pits and scratches, and those that are durophagous (such as feeding on seeds) have many pits (Fig. 6) and sometimes have enamel 'spalling' (Schubert & Ungar 2005) which we did not observe. Few mammals feed habitually on gymnosperms and pteridophytes, and to our knowledge no pit-to-scratch ratios were constructed in studies on these mammals (Puech et al. 1986; Michaux et al. 2008), making direct comparisons difficult. Though the diets of juvenile *Trilophosaurus buettneri* and *Trilophosaurus phasmalophos* were clearly less hard than that of the unnamed taxon (PEFO 43837), they were nonetheless harder and tougher than would likely be seen if primarily feeding on ferns or other 'soft' vegetation (Fig. 6). Additionally, while we focused on aboveground vegetation, we cannot currently rule out the possibility of trilophosaurids including roots or tubers in their diet.

5.3. Comparison of methodology

The relative similarity of ratios for both specimens of *Trilophosaurus phasmalophos* despite the differing counting methods indicates that both strategies (method 1 and method 2) may be viable in determining pit-to-scratch ratios. *Trilophosaurus buettneri* (SMU 77695, including the mesial side) differed from the more similar *Trilophosaurus phasmalophos* specimen (DMNH PAL 2018-05-0012) by roughly twice the difference in pit-to-scratch ratio that each *Trilophosaurus phasmalophos* specimen differed from each other. However, given the very small sample sizes, larger sample sizes may be necessary to unequivocally confirm these observations.

5.4. Microwear orientation implications for jaw closure mechanics

Of the few Triassic reptiles subject to dental microwear analysis prior to this study, all that investigated jaw movement recovered evidence of orthal jaw closure (Goswami et al. 2005; Kubo & Kubo 2014), and importantly this includes azendohsaurid allokotosaurs (Goswami et al. 2005). Azendohsaurids are consistently recovered as the sister group to trilophosaurids (e.g., Nesbitt et al. 2022), suggesting that orthal jaw closure is the plesiomorphic state in Allokotosauria. Our study provides evidence for jaw closure mechanics from dental microwear in the genus *Trilophosaurus*. Several authors (i.e., Parks 1969; Demar & Bolt 1981) have remarked on the occasional presence of wear facets primarily on the central but also rarely all three cusps in some *Trilophosaurus buettneri* dentition, in a configuration suggesting (in conjunction with some aspects of the cranium and implied musculature) that they exhibited strictly orthal processing.

Despite these wear facets, the microwear signal from *Trilophosaurus buettneri* is not primarily orthal. When looking at feature angles from all sides of the teeth there is no predominant direction (Fig. 5f). Labial and lingual sites of analysis, though from different teeth, both indicate orthal movement with their apically-directed features and low standard deviations, but the distal side of the distal-most tooth has features with large standard deviations primarily directed labially and with one site directed lingually. In contrast, the mesial side of the distal-most tooth has features directed labially, lingually, and apically, in addition to adjacent sites of analysis contrasting with each other (see above). Because of the software used here, only the mean feature orientation was available for our analysis, which obscures the true directions of features in this study. This could result in mean feature directions at a diagonal angle when in fact they occurred bimodally apically and labio-lingually, and this could explain our large standard deviations (indeed six of the eight mean feature directions for *Trilophosaurus phasmalophos* [DMNH PAL 2018-05-0012] are within 15º of 45º or 135º and four of the ten mesial and distal side mean feature directions for *Trilophosaurus buettneri* are within 20º of 45º or 135º).

Given these lines of evidence, two scenarios for jaw movement present themselves: [1] jaw closure is not exclusively orthal, and wear facets are only reflective of one plane of motion; [2] jaw closure is exclusively orthal, and scratch orientation signals are not reflective of jaw closure mechanics.

In scenario [1], *Trilophosaurus buettneri* exhibits jaw movement either directly producing diagonal scratches or producing scratches both apico-basally and labio-lingually. This could occur via either transverse movement of the mandible or via cranial kinesis. Kinesis is considered unlikely because although the sutures of the skull have not been directly described the skull of *Trilophosaurus* has been consistently referred to as robust (Gregory 1945; Spielmann et al. 2008), a trait not associated with kinesis. Gregory (1945) considered transverse movement of the mandible unlikely because the quadrate condyle is laterally expanded; however, this conclusion may be premature: Varriale (2016) suggested *Leptoceratops* (a dinosaur with a beak and akinetic skull) exhibited ortho-palinal jaw movement based on microwear. They concluded that because there is a lack of kinesis the quadrate-articular joint must be the source of that motion, despite prior assumptions of exclusively orthal movement. If correct this suggests that our focus on modern analogs may be limiting our ability to recognize alternative methods of jaw-flexion. Research into the quadrate-articular joint of trilophosaurids and more detailed study of microwear direction on a larger sample size of teeth are necessary to further this hypothesis. Further study of the wear facets of *Trilophosaurus buettneri* and the specifics of tooth interdigitation are necessary before an explanation of their apparently exclusively orthal formation can be proposed.

In scenario [2] the microwear signal is not indicative of jaw movement. Although microwear scratch orientations have proven to be a strong indicator of jaw movement in mammals (Ungar 2015) this hypothesis has not been tested in reptiles, and even they may not be relevant to *Trilophosaurus* given the lack of modern analogs bearing similar jaw anatomy (i.e., jaws with mesial edentulism and distal labio-lingually broad dentition). The unique shape of the teeth may result in food moving in unexpected ways despite only orthal movement of the jaw, although this would need to be investigated with digital or physical models to be confirmed. This hypothesis better explains the presence of one or three wear facets found on some *Trilophosaurus buettneri* teeth that are apically directed, and the lack of transverse wear facets. Though

both scenarios are possible, we consider the second to be more likely for *Trilophosaurus buettneri*.

Both scenario [1] and [2] can be applied to *Trilophosaurus phasmalophos* (DMNH PAL 2018-05-0012), which has features primarily directed lingually and only differing at the very base and very top (Fig. 5a). Because our work is the first to describe cranial material of the species, the likelihood of cranial kinesis or lateral quadrate-articular movement is unknown. Given the lack of wear facets, we consider these scenarios to be equally likely. In the unnamed taxon, the clearly concave wear facets indicate that jaw movement is likely exclusively orthal because these facets fit well with the shape of the presumably interdigitating opposing teeth, and no transverse wear facets are known. More research into the craniomandibular system (ideally using CT scanning), the quadrate-articular joint, the scratch orientations of all species across individuals and purported age classes, and physical or virtual modelling of tooth occlusion and food movement across the teeth will be important steps in determining which scenario is correct.

5.5. Broader significance

Given the somewhat frequent occurrence of *Trilophosaurus buettneri* in Upper Triassic sediments compared to other trilophosaurids (Spielmann et al. 2008), it is interesting to note the relative similarity of the pit-to-scratch ratios in this species occurring before the Adamanian-Revueltian boundary to *Trilophosaurus phasmalophos* occurring after it. The resolution of our results is insufficient to determine what specific plant taxa they were consuming, and differences in tooth shape and direction of wear suggest there may be some differences in the diet, but these differences do not appear to constitute a radical change (i.e., they remained tough-semihard browsers). This suggests that specific plant taxa preferred in *Trilophosaurus* diets may span the proposed boundary. Additionally, the presence of a temporally and spatially co-occurring taxon with clearly divergent pit-to-scratch ratios indicates the potential for dietary niche partitioning between immature *Trilophosaurus buettneri* and the unnamed taxon (PEFO 43837) in the Adamanian assemblages, and potentially that the unnamed taxon relied on plants that did not survive this boundary. Because this taxon is currently not reported from the SMU v572 locality, it is not presently clear if teeth from *Trilophosaurus buettneri* in the same geographic location as the new taxon will exhibit the same pattern; however, they are known to cooccur at PFV 456. Ontogenetic niche partitioning is known – and indeed considered integral to the success of – living crocodylians and squamates, and has been suggested for some extinct archosaurs (Werner & Gilliam 1984; Bestwick et al. 2020). This has also been suggested previously for *Trilophosaurus buettneri*, given the difference in form between immature and adult teeth (Parks 1969; Demar & Bolt 1981), and our results indicate this could be the case considering the dissimilarity between the *Trilophosaurus buettneri* specimen we investigated (SMU 77695) and the unnamed taxon (PEFO 43837), which, while not conspecific, has teeth that are morphologically similar to adult *Trilophosaurus buettneri*. To fully test this, a comprehensive analysis of dental microwear across an ontogenetic spectrum of *Trilophosaurus buettneri* dentitions is necessary, but is currently not available.

Plant species that are known from stratigraphically equivalent sites include ferns, cycads, horsetails, and a variety of conifer trees (Savidge 2007; Kustatscher et al. 2018). Late Triassic horsetails likely still possessed phytoliths (Carter 1999), which could have resulted in the apical wear facets of adult *Trilophosaurus buettneri* if the phytoliths are of a similar size to living horsetails, or if larger they could potentially explain the pits on the teeth. The toughness of these forms is also unknown, which make them, alongside the likely tough cycads and trees, possible sources of the high microwear feature density (from significant oral processing). Evidence from muscle attachments and claw shape suggest that *Trilophosaurus buettneri* may have been scansorial (Gregory 1945; Heckert et al. 2005), a hypothesis that may be further supported by the shape of the semicircular canal in this taxon (Bronzati et al. 2021); scansoriality may have facilitated uptake of the aforementioned plant taxa by *Trilophosaurus buettneri.* The relative lack of modern animals that feed on non-angiosperm plant tissues means that few studies have been able to determine the potential metabolizable energy of these tissues, but an experiment using sheep rumen fluid found the modern *Gingko biloba, Araucaria araucana, Equisetum* spp., some conifers, and some ferns to have similar energy content to the diet of modern herbivores (with other ferns, tree ferns, podocarp conifers, and cycads having lower energy content) (Hummel et al. 2008). Given the high diversity of fossils of conifer trees in Petrified Forest National Park (Savidge 2007), and the high potential energy of these as botanical uptake (Hummel et al. 2008), the skeletal traits and dental microwear features in trilophosaurids tentatively support hypotheses of specialized arboreal herbivory in this group comparable to the modern-day green iguana (*Iguana iguana*) (Heckert et al. 2005). Counterpoints to this hypothesis are that although their teeth do not have a modern analog, several extinct taxa that exhibit similar dentition are not thought to be scansorial (e.g., *Palacrodon*, some Procolophonidae, Polyglyphanodontidae (Sues & Olsen 1993; Nydam & Cifelli 2005)). Furthermore, the potential of high dust/grit content suggested by our findings would better support a diet consistent with life on the ground (Ungar et al. 1995).

Trilophosaurids (alongside aetosauriforms, silesaurids, and dicynodonts) are one of the few reported medium-to-large-bodied potentially herbivorous tetrapod taxa known from Norian communities in southwestern North America (Heckert 2004; Nesbitt & Stocker 2008). The Late Triassic terrestrial vertebrate communities of North America have been suggested to be trophically "unbalanced" because large-bodied carnivores outnumber herbivores in recovered abundance and diversity (Heckert 2004; Nesbitt & Stocker 2008; Drumheller et al. 2014), highlighting the need to examine the dietary ecology of putatively herbivorous components of these assemblages to build a comprehensive understanding of these possibly unusual communities. Classically, the majority of individuals, biomass, and often diversity, are within the herbivore component of animal communities, and predators account for much less of modern terrestrial ecosystems (Schmitz 2008; Tucker & Rogers 2014; Fløjgaard et al. 2022). This is understood to relate to the trophic inefficiency inherent in animal biology, where on average only 10% of the energy from a given trophic level (like herbivores) can be passed to the next level (like primary predators) (Lindeman 1942). Herbivore abundance and diversity also relate to the relative ubiquity and diversity of plant life and therefore dietary niches available to herbivores (Tucker & Rogers 2014). On average, the more general the diet of an herbivore is the more competition it is likely to face, encouraging dietary niche partitioning and therefore greater speciation (Belovsky 1986). Some Chinle Formation assemblages do not seem to follow these patterns for diversity and biomass, challenging understandings of terrestrial trophic efficiency. However, other research has challenged these assumptions about atypical community composition, citing historical collection and identification biases towards large well-preserved taxa that artificially limit the described species pool in this and other formations (Nesbitt & Stocker 2008; Brown et al. 2013). In a similar case from the Cretaceous Period, taphonomic processes were considered a significant influence on what trophic levels were preserved (Läng et al. 2013). Data presented herein demonstrate the cooccurrence of sampled trilophosaurid specimens from vertebrate assemblages including other putative herbivores, the vast majority of which are medium-to-large bodied aetosauriforms. The PFV 456 assemblage exemplifies this pattern, where at least two trilophosaurid taxa are present (*Trilophosaurus buettneri* and the unnamed taxon, PEFO 43837), alongside six taxa of medium-to-large bodied aetosauriforms (*Revueltosaurus callenderi*, *Acaenasuchus geoffreyi*, *Calyptosuchus wellesi*, *Adamanasuchus eisenhardtae*, *Tecovasuchus chatterjeei*, and *Desmatosuchus spurensis*); this, alongside our evidence for probable niche-space partitioning in the trilophosaurid taxa, suggests the herbivorous elements of this ecosystem were relatively diverse, contrary to the hypotheses of depauperate herbivorous components in Chinle ecosystems (Heckert 2004; Nesbitt & Stocker 2008; Drumheller et al. 2014) and further supported by the findings of Singh et al. (2021). Differing taphonomic pathways or collection methods may account for these differences, or alternatively this may be caused by changes in community composition over the ~20 Ma timeframe of Late Triassic deposition in the Chinle Formation and Dockum Group. Evidence for likely niche-space partitioning in trilophosaurid taxa sampled herein raises the question of whether aetosauriforms (the most diverse group of likely herbivores in these strata) also evolved divergent herbivory strategies; analysis of dental microwear in aetosauromorph dentitions could further understandings of niche-space partitioning amongst herbivorous taxa in these communities.

Several key avenues of research present themselves following the results of this study. Dental Microwear Topographic Analysis of these and other trilophosaurids would help to provide other quantitative measures to understand the differences within and between species (as recommended by Bestwick et al. 2019; Winkler et al. 2019; Bestwick et al. 2020). We also suggest computational and/or physical modelling of teeth like those found in *Trilophosaurus* to better understand how food moves across these teeth, and more detailed descriptions of the jaw joint and posterior sections of the skull will help us to understand if the wear patterns observed are from transverse jaw movement or other factors. Sampling more age classes (and quantitative confirmation of these classes) and greater sample sizes will help to determine the significance of these and future findings, as well as elucidating potential intraspecific, annual, and tooth-row variation in diet signal (Ungar 2015). Future researchers are encouraged to test our results using dental microwear derived from tooth molds to remove debris that cannot effectively be removed by direct cleaning.

6. Conclusion

The trilophosaurids *Trilophosaurus phasmalophos* (DMNH PAL 2018-05-0012) and an immature example of *Trilophosaurus buettneri* (SMU 77695) exhibit dental microwear directions at odds with past hypotheses of jaw closure mechanics within the group. Additionally, the feature counts and differences in pit-to-scratch ratios may suggest some of the first direct evidence for herbivorous niche partitioning in closely related species in the Late Triassic American Southwest (between *Trilophosaurus buettneri* and an unnamed taxon (PEFO 43837)). The relative similarity of microwear between *Trilophosaurus buettneri* (SMU 77695) and *Trilophosaurus phasmalophos* (PEFO 42082, DMNH PAL 2018-05-0012) suggests that

some aspects of the botanical ecosystem may have been unaffected by the Adamanian-Revueltian boundary.

Acknowledgements

We thank members of the PEFO and Virginia Tech field teams for their fieldwork efforts in 2018 and 2019. R. Mueller and J. Socha facilitated μCT scanner access at Virginia Tech. A. Marsh, W. Parker, M. Smith, D. Wagner, D. Boudreau, and P. Varela prepared PEFO specimens and facilitated access to the PEFO collections. We thank A. Marsh and W. Parker for discussions of scientific content and fieldwork support. S. Xiao provided SEM access at Virginia Tech. We thank C. Sidor, K. Anderson, B. Gee, and E. Smith, and the University of Washington Burke Museum field group for collecting, preparing, and facilitating access to UMBW 116791. D. Winkler facilitated access to SMU 77695. M. Brown and W. Reyes facilitated access to TMM 31099-15 and photographed TMM specimens. P. Ungar provided access to the Microware software. This study was supported by the David R. Wones Geological Scholarship (to BTK), the USA National Park Service (PMIS 209814 to BTK), the Virginia Tech Department of Geosciences (to BTK, MRS, and SJN), the National Science Foundation (EAR 1943286 to SJN), the David B. Jones Foundation (to MRS, SJN, and MPM), and the Petrified Forest Museum Association (to BTK). We thank S. Chambi-Trowell and J. Cisneros for reviewing the manuscript. This is Petrified Forest Paleontological Contribution No. 92; the opinions presented herein are those of the authors and do not represent the views of the United States government.

7. References

Atchley, S. C., Nordt, L. C., Dworkin, S. I ., Ramezani, J., Parker, W. G., Ash, S. R. & Bowring, S. A. (2014): A linkage among pangean tectonism, cyclic alluviation, climate change, and biologic turnover in the Late Triassic: the record from the Chinle Formation, southwestern United States. – Journal of Sedimentary Research, **83**: 1147–1161.

Baranyi, V., Reichgelt, T., Olsen, P. E., Parker, W. G. & Kürschner, W. M. (2018): Norian vegetation history and related environmental changes: New data from the Chinle Formation, Petrified Forest National Park (Arizona, SW USA). – GSA Bulletins, **130**: 775–795.

Belovsky, G. E. (1986): Generalist herbivore foraging and its role in competitive interactions. – American Zoologist, **26**: 51–69.

Benton, M. J. (1984): Tooth form, growth, and function in Triassic rhynchosaurs. – Palaeontology, **27**: 737–776.

Bestwick, J., Jones, A. S., Purnell, M. A. & Butler, R. J. (2021): Dietary constraints of phytosaurian reptiles revealed by dental microwear textural analysis. – Paleontology, **64**: 119–136.

Bestwick, J., Unwin, D. M., Butler, R. J. & Purnell, M. A. (2020): Dietary diversity and evolution of the earliest flying vertebrates revealed by dental microwear texture analysis. – Nature Communications, **11**: 5293.

Bestwick, J., Unwin, D. M. & Purnell, M. A. (2019): Dietary differences in archosaur and lepidosaur reptiles revealed by dental microwear textural analysis. – Scientific Reports, **9**: 11691.

Bronzati, M., Benson, R. B. J., Evers, S. W., Ezcurra, M. D., Cabreira, S. F., Choiniere, J., Dollman, K. N., Paulina-Carabajal, A., Radermacher, V. J., Roberto-da-Silva, L., Sobral, G., Stocker, M. R., Witmer, L. M., Langer, M. C. & Nesbitt, S. J. (2021): Deep evolutionary diversification of semicircular canals in archosaurs. – Current Biology, **31**: 2520–2529.e6.

Brown, C. M., Evans, D. C., Campione, N. E., O'Brien, L. J. & Eberth, D. A. (2013): Evidence for taphonomic size bias in the Dinosaur Park Formation (Campanian, Alberta), a model Mesozoic terrestrial alluvial-paralic system. – Palaeogeography, Palaeoclimatology, Palaeoecology, **372**: 108–122.

Carter, J. A. (1999): Later Devonian, Permian, and Triassic phytoliths from Antarctica. – Micropaleontology, **45**: 56–61.

Case, E. C. (1928a): A Cotylosaur from the Upper Triassic of western Texas. – Journal of the Washington Academy of Sciences, **18**: 177–178.

Case, E. C. (1928b): Indications of a cotylosaur and of a new form of fish from the Triassic beds of Texas, with remarks on the Shinarump Conglomerate. – Contributions from the University of Michigan Museum of Paleontology, **3**: 1–14.

Chambi-Trowell, S. A. V., Whiteside, D. I., Skinner, M., Benton, M. J. & Rayfield, E. J. (2022): Phylogenetic relationships of the European trilophosaurids *Tricuspisaurus thomasi* and *Variodens inopinatus*. – Journal of Vertebrate Paleontology, **41**: e1999250.

Covert, H. H. & Kay, R. F. (1981): Dental microwear and diet: Implications for determining the feeding behaviors of extinct primates, with a comment on the dietary pattern of Sivapithecus. – American Journal of Physical Anthropology, **55**: 331–336.

Demar, R. & Bolt, J. R. (1981): Dentitional organization and function in a Triassic reptile. – Journal of Paleontology, **55**: 967–984.

Drumheller, S. K., Stocker, M. R. & Nesbitt, S. J. (2014): Direct evidence of trophic interactions among apex predators in the Late Triassic of western North America. – Naturwissenschaften, **101**: 975–987.

Drymala, S. M., Bader, K. & Parker, W. G. (2021): Bite marks on an aetosaur (Archosauria, Suchia) osteoderm: assessing late Triassic predator-prey ecology through ichnology and tooth morphology. – Palaios, **36**: 28–37.

Dubiel, R. F. (1994): Triassic deposystems, paleogeography, and paleoclimate of the western interior. In: Caputo, M. V., Peterson, J. A. & Franczyk, K. J. (eds.): Mesozoic Systems of the Rocky Mountain Region, USA: 133–168; Denver (Rocky Mountain Section of SEPM).

Ezcurra, M. D. & Butler, R. J. (2018): The rise of the ruling reptiles and ecosystem recovery from the Permo-Triassic mass extinction. – Proceedings of the Royal Society B: Biological Sciences, **285**: 20180361.

Fiorillo, A. R. (1998): Dental micro wear patterns of the sauropod dinosaurs *Camarasaurus* and *Diplodocus*: Evidence for resource partitioning in the late Jurassic of North America. – Historical Biology, **13**: 1–16.

Fløjgaard, C., Pedersen, P. B. M., Sandom, C. J., Svenning, J.-C. & Ejrnæs, R. 2022: Exploring a natural baseline for large-herbivore biomass in ecological restoration. – Journal of Applied Ecology, **59**: 18–24.

Flynn, J. J., Nesbitt, S. J., Parrish, J. M., Ranivoharimanana, L. & Wyss, A. R. (2010): A new species of *Azendohsaurus* (Diapsida: Archosauromorpha) from the Triassic Isalo Group of southwestern Madagascar: Cranium and mandible. – Palaeontology, **53**: 669–688.

Gere, K., Bodor, E. R., Makádi, L. & Ősi, A. (2021): Complex food preference analysis of the Late Cretaceous (Santonian) lizards from Iharkút (Bakony Mountains, Hungary). – Historical Biology, **33**: 3686–3702.

Gonçalves, G. S. & Sidor, C. A. (2019): A new drepanosauromorph, *Ancistronychus paradoxus* n. gen. et sp., from the Chinle Formation of Petrified Forest National Park, Arizona, USA. – PaleoBios, **36**: 1–10.

Gordon, K. D. (1984): The assessment of jaw movement direction from dental microwear. – American Journal of Physical Anthropology, **63**: 77–84.

Gordon, K. D. (1988): A review of methodology and quantification in dental microwear analysis. – Scanning Microscopy, **2**: 1139–1147.

Goswami, A., Flynn, J. J., Ranivoharimanana, L. & Wyss, A. R. (2005): Dental microwear in Triassic amniotes: implications for paleoecology and masticatory mechanics. – Journal of Vertebrate Paleontology, **25**: 320–329.

Gregory, J. T. (1945): Osteology and relationships of *Trilophosaurus*. – University of Texas Publications, **4401**: 273–359.

Grine, F. E., Ungar, P. S. & Teaford, M. F. (2002): Error rates in dental microwear quantification using scanning electron microscopy. – Scanning, **24**: 144–153.

Heckert, A. B. (2004): Late Triassic microvertebrates from the lower Chinle Group (Otischalkian-Adamanian:Carnian), southwestern U.S.A. – Bulletins of the New Mexico Museum of Natural History and Science, **27**: 177 pp.

Heckert, A. B., Lucas, S. G., Rinehart, L. F., Spielmann, J. A., Hunt, A. P. & Kahle, R. (2006): Revision of the archosauromorph reptile Trilophosaurus, with a description of the first skull of *Trilophosaurus jacobsi*, from the Upper Triassic Chinle Group, west Texas, USA. – Palaeontology, **49**: 621–640.

Heckert, A. B., Spielmann, J. A. & Lucas, S. G. (2005): The Late Triassic archosauromorph *Trilophosaurus* as an arboreal climber. – Rivista Italiana di Paleontologia e Stratigrafa, **111**: 395–412.

Hedberg, C. & DeSantis, L. R. G. (2017): Dental microwear texture analysis of extant koalas: clarifying causal agents of microwear. – Journal of Zoology, **301**: 206–214.

Holwerda, F. M., Beatty, B. L. & Schulp, A. S. (2013): Dental macro- and microwear in *Carinodens belgicus*, a small mosasaur from the type Maastrichtian. – Netherlands Journal of Geosciences, **92**: 267–274.

Huene, F. v. (1932): Die fossile Reptil-Ordnung Saurischia: ihre Entwicklung und Geschichte. Leipzig (Borntraeger).

Hummel, J., Gee, C. T., Südekum, K.-H., Sander, P. M., Nogge, G. & Clauss, M. (2008): In vitro digestibility of fern and gymnosperm foliage: implications for sauropod feeding ecology and diet selection. – Proceedings of the Royal Society, B: Biological Sciences, **275**: 1015–1021.

Irmis, R. B., Nesbitt, S. J., Padian, K., Smith, N. D., Turner, A. H., Woody, D. & Downs, A. (2007): A Late Triassic dinosauromorph assemblage from New Mexico and the rise of dinosaurs. – Science, **317**: 358–361.

King, T., Andrews, P. & Boz, B. (1999): Effect of taphonomic processes on dental microwear. – American Journal of Physical Anthropology, **108**: 359–373.

Kligman, B. T., Marsh, A. D., Nesbitt, S. J., Parker, W. G. & Stocker, M. R. (2020a): New trilophosaurid species demonstrates a decline in allokotosaur diversity across the Adamanian-Revueltian boundary in the Late Triassic of western North America. – Palaeodiversity, **13**: 25–37.

Kligman, B. T., Marsh, A. D., Sues, H.-D. & Sidor, C. A. (2020b): A new non-mammalian eucynodont from the Chinle Formation (Triassic: Norian), and implications for the early Mesozoic equatorial cynodont record. – Biology Letters, **16**: 20200631.

Kubo, M. O. & Yamada, E. (2014): The inter-relationship between dietary and environmental properties and tooth wear: Comparisons of mesowear, molar wear rate, and hypsodonty index of extant sika deer populations. – PLOS ONE, **9**: e90745.

Kubo, T. & Kubo, M. O. (2014): Dental microwear of a Late Triassic dinosauriform, *Silesaurus opolensis*. – Acta Palaeontologica Polonica, **59**: 305–312.

Kubo, T., Zheng, W., Kubo, M.O. & Jin, X. (2021): Dental microwear of a basal ankylosaurine dinosaur, *Jinyunpelta* and its implication on evolution of chewing mechanism in ankylosaurs. – PLOS ONE, **16**: e0247969.

Kustatscher, E., Ash, S. R., Karasev, E., Pott, C., Vajda, V., Yu, J. & McLoughlin, S. (2018): Flora of the Late Triassic. In: Tanner, L. H. (eds.): The Late Triassic World. – Topics in Geobiology: 545–622; Cham (Springer).

Läng, E., Boudad, L., Maio, L., Samankassou, E., Tabouelle, J., Tong, H. & Cavin, L. (2013): Unbalanced food web in a Late Cretaceous dinosaur assemblage. – Palaeogeography, Palaeoclimatology, Palaeoecology, **381–382**: 26–32.

Lepre, C. J. & Olsen, P. E. (2021): Hematite reconstruction of Late Triassic hydroclimate over the Colorado Plateau. – Proceedings of the National Academy of Sciences, **118**: e2004343118.

Lessner, E. J., Parker, W. G., Marsh, A. D., Nesbitt, S. J., Irmis, R. B. & Mueller, B. D. (2018): New insights into Late Triassic dinosauromorph-bearing assemblages from Texas using apomorphy-based identifications. – PaleoBios, **35**.

Lindeman, R. L. (1942): The trophic-dynamic aspect of ecology. – Ecology, **23**: 399–417.

Mallon, J. C. & Anderson, J. S. (2014): The functional and palaeoecological implications of tooth morphology and wear for the megaherbivorous dinosaurs from the Dinosaur Park Formation (Upper Campanian) of Alberta, Canada. – PLOS ONE, **9**: e98605.

Mannion, P. D., Upchurch, P., Carrano, M. T. & Barrett, P. M. (2011): Testing the effect of the rock record on diversity: A multidisciplinary approach to elucidating the generic richness of sauropodomorph dinosaurs through time. – Biological Reviews, **86**: 157–181.

Marsh, A. D., Parker, W. G., Nesbitt, S. J., Kligman, B. T. & Stocker, M. R. (2022): *Puercosuchus traverorum* n. gen. and sp.: a new malerisaurine azendohsaurid (Archosauromorpha: Allokotosauria) from two monodominant bonebeds in the Chinle Formation (Upper Triassic, Norian) of Arizona. – Journal of Paleontology, **96**: 1–39.

Marsh, A. D., Smith, M. E., Parker, W. G., Irmis, R. B. & Kligman, B. T. (2020): Skeletal anatomy of *Acaenasuchus geoffreyi* Long and Murry, 1995 (Archosauria: Pseudosuchia) and its implications for the origin of the aetosaurian carapace. – Journal of Vertebrate Paleontology, **40**: e1794885.

Martz, J. W. (2008): Lithostratigraphy, chemostratigraphy, and vertebrate biostratigraphy of the Dockum Group (Upper Triassic), of southern Garza County, West Texas. – PhD thesis, Texas Tech University, 461 pp.

Martz, J. W., Mueller, B., Nesbitt, S. J., Stocker, M. R., Parker, W. G., Atanassov, M., Fraser, N., Weinbaum, J. & Lehane, J. R. (2012): A taxonomic and biostratigraphic re-evaluation of the Post Quarry vertebrate assemblage from the Cooper Canyon Formation (Dockum Group, Upper Triassic) of southern Garza County, western Texas. – Earth and Environmental Science Transactions of the Royal Society of Edinburgh, **103**: 339–364.

Martz, J. W. & Parker, W. G. (2017): Revised formulation of the Late Triassic land vertebrate "faunachrons" of western North America: recommendations for codifying nascent systems of vertebrate biochronology. In: Zeigler, K. E. & Parker, W. G. (eds.): Terrestrial Depositional Systems: 39–125; Elsevier.

Michaux, J., Hautier, L., Simonin, T. & Vianey-Liaud, M. (2008): Phylogeny, adaptation and mandible shape in Sciuridae (Rodentia, Mammalia). – Mammalia, **72**: 286–296.

Mihlbachler, M. & Beatty, B. (2012): Magnification and resolution in dental microwear analysis using light microscopy. – Palaeontologia Electronica, **15**: 25a.

Mihlbachler, M. C., Foy, M. & Beatty, B. L. (2019): Surface replication, fidelity and data loss in traditional dental microwear and dental microwear texture analysis. – Scientific Reports, **9**: 1595.

Mueller, B. D. (2016): Triassic tetrapod paleontology and taphonomy of the Boren Quarry, Dockum Group, Garza County, Texas. – PhD thesis, Texas Tech University, 300 pp.

Mueller, B. D. & Parker, W. (2006): A new species of *Trilophosaurus* (Diapsida: Archosauromorpha) from the Sonsela Member (Chinle Formation) of Petrified Forest National Park, Arizona. – Museum of Northern Arizona Bulletins, **62**: 119–125.

Murry, P. A. (1987): New reptiles from the Upper Triassic Chinle Formation of Arizona. – Journal of Paleontology **61**: 773–786.

Nesbitt, S. J., Flynn, J. J., Pritchard, A. C., Parrish, J. M., Ranivoharimanana, L. & Wyss, A. R. (2015): Postcranial Osteology of *Azendohsaurus madagaskarensis* (?Middle to Upper Triassic, Isalo Group, Madagascar) and its systematic position among stem archosaur reptiles. – Bulletins of the American Museum of Natural History, **2015**: 1–126.

Nesbitt, S. J., Sidor, C. A., Irmis, R. B., Angielczyk, K. D., Smith, R. M. H. & Tsuji, L. A. (2010): Ecologically distinct dinosaurian sister group shows early diversification of Ornithodira. – Nature, **464**: 95–98.

Nesbitt, S. J. & Stocker, M. R. (2008): The vertebrate assemblage of the Late Triassic Canjilon Quarry (Northern New Mexico, USA), and the importance of apomorphy-based assemblage comparisons. – Journal of Vertebrate Paleontology, **28**: 1063–1072.

Nesbitt, S. J., Stocker, M. R., Ezcurra, M. D., Fraser, N. C., Heckert, A. B., Parker, W. G., Mueller, B., Sengupta, S., Bandyopadhyay, S., Pritchard, A. C. & Marsh, A. D. (2022): Widespread azendohsaurids (Archosauromorpha, Allokotosauria) from the Late Triassic of western USA and India. – Papers in Palaeontology, **8**: e1413.

Nordt, L., Atchley, S. & Dworkin, S. (2015): Collapse of the Late Triassic megamonsoon in western equatorial Pangea, present-day American Southwest. – Geological Society of America Bulletins, **127**: 1798–1815.

Nydam, R. L. & Cifelli, R. L. (2005): New data on the dentition of the scincomorphan lizard *Polyglyphanodon sternbergi*. – Acta Palaeontologica Polonica, **50**: 73–78.

Ősi, A. (2011): Feeding-related characters in basal pterosaurs: implications for jaw mechanism, dental function and diet. – Lethaia, **44**: 136–152.

Ősi, A., Barrett, P. M., Földes, T. & Tokai, R. (2014): Wear pattern, dental function, and jaw mechanism in the Late Cretaceous ankylosaur Hungarosaurus. – The Anatomical Record, **297**: 1165–1180.

Ősi, A. & Weishampel, D. B. (2009): Jaw mechanism and dental function in the late cretaceous basal eusuchian *Iharkutosuchus*. – Journal of Morphology, **270**: 903–920.

Padian, K. & Sues, H.-D. (2015): Great Transformations in Vertebrate Evolution. Chicago (University of Chicago Press.)

Parker, W. G. (2005): A new species of the Late Triassic aetosaur *Desmatosuchus* (Archosauria: Pseudosuchia). – Comptes Rendus Palevol, **4**: 327–340.

Parker, W. G. & Martz, J. W. (2010): The Late Triassic (Norian) Adamanian–Revueltian tetrapod faunal transition in the Chinle Formation of Petrified Forest National Park, Arizona. – Earth and Environmental Science Transactions of the Royal Society of Edinburgh, **101**: 231–260.

Parker, W. G., Nesbitt, S. J., Marsh, A. D., Kligman, B. T. & Bader, K. (2021): First occurrence of *Doswellia* cf. *D. kaltenbachi* (Archosauriformes) from the Late Triassic (middle Norian) Chinle Formation of Arizona and its implications on proposed biostratigraphic correlations across North America during the Late Triassic. – Journal of Vertebrate Paleontology, **41**: e1976196.

Parks, P. (1969): Cranial anatomy and mastication of the Triassic reptile *Trilophosaurus*. – Master's thesis, University of Texas at Austin, 89 pp.

Pinto Llona, A. C. (2006): Comparative dental microwear analysis of cave bears *Ursus spelaeus* Rosenmüller, 1794 and brown bears *Ursus arctos* Linnaeus, 1748. – Scientific Annals, School of Geology, Aristotle University of Thessaloniki, **98**: 103–108.

Pritchard, A.C. & Sues, H.-D. (2019): Postcranial remains of *Teraterpeton hrynewichorum* (Reptilia: Archosauromorpha) and the mosaic evolution of the saurian postcranial skeleton. – Journal of Systematic Palaeontology, **17**: 1745–1765.

Puech, P., Cianfarani, F. & Albertini, H. (1986): Dental microwear features as an indicator for plant food in early hominids: A preliminary study of enamel. – Human Evolution, **1**: 507–515.

Ramezani, J., Hoke, G. D., Fastovsky, D. E., Bowring, S. A., Therrien, F., Dworkin, S. I., Atchley, S. C. & Nordt, L. C. (2011): High-precision U-Pb zircon geochronology of the Late Triassic Chinle Formation, Petrified Forest National Park (Arizona, USA): Temporal constraints on the early evolution of dinosaurs. – GSA Bulletins, **123**: 2142–2159.

Rasmussen, C., Mundil, R., Irmis, R. B., Geisler, D., Gehrels, G. E., Olsen, P. E., Kent, D. V., Lepre, C., Kinney, S. T., Geissman, J. W. & Parker, W. G. (2021): U-Pb zircon geochronology and depositional age models for the Upper Triassic Chinle Formation (Petrified Forest National Park, Arizona, USA): Implications for Late Triassic paleoecological and paleoenvironmental change. – GSA Bulletins, **133**: 539–558.

Rivera-Sylva, H., Barron-Ortiz, C., González, R., Rodríguez, R., Guzman Gutierrez, J. R., Valdéz, F., Dávila, C., Potosí, L. & Potosí, S. (2019): Preliminary assessment of hadrosaur dental microwear from the Cerro del Pueblo Formation of Coahuila, Mexico Preliminary assessment of hadrosaur dental microwear from the Cerro del Pueblo Formation (Upper Cretaceous: Campanian) of Coahuila, northeastern Mexico. – Paleontología Mexicana, **8**: 17–28.

Robinson, P. L. (1957): An unusual sauropsid dentition. – Journal of the Linnean Society of London, Zoology, **43**: 283–293.

Savidge, R. A. (2007): Wood anatomy of Late Triassic trees in Petrified Forest National Park, Arizona, USA, in relation to *Araucarioxylon arizonicum* Knowlton, 1889. – Bulletin of Geosciences, **82**: 301–328.

Schmitz, O. J. (2008): Herbivory from individuals to ecosystems. – Annual Review of Ecology, Evolution, and Systematics, **39**: 133–152.

Schubert, B. W. & Ungar, P. S. (2005): Wear facets and enamel spalling in tyrannosaurid dinosaurs. – Acta Palaeontologica Polonica, **50**: 93–99.

Sengupta, S., Ezcurra, M. D. & Bandyopadhyay, S. (2017): A new horned and long-necked herbivorous stem-archosaur from the Middle Triassic of India. – Scientific Reports, **7**: 8366.

Simpson, G. G. (1926): Mesozoic Mammalia, IV; The multituberculates as living animals. – American Journal of Science, **s5–11**: 228–250.

Singh, S. A., Elsler, A., Stubbs, T. L., Bond, R., Rayfield, E. J. & Benton, M. J. (2021): Niche partitioning shaped herbivore macroevolution through the early Mesozoic. – Nature Communications, **12**: 2796.

Spielmann, J. A., Lucas, S. G., Heckert, A. B., Rinehart, L. F. & Hunt, A. P. (2007): Taxonomy and biostratigraphy of the Late Triassic archosauromorph *Trilophosaurus*. In: Lucas, S. G. & Spielmann, J. A. (eds.): Triassic of the American West. – Bulletins of the New Mexico Museum of Natural History and Science, **40**: 231–240.

Spielmann, J. A., Lucas, S. G., Rhinehart, L. F. & Heckert, A. B. (2008): The Late Triassic archosauromorph *Trilophosaurus*. – Bulletins of the New Mexico Museum of Natural History and Science, **43**: 192 pp.

Stocker, M. R. (2013): Conceptualizing vertebrate faunal dynamics : new perspectives from the Triassic and Eocene of Western North America. – PhD thesis, University of Texas at Austin, 297 pp.

Stocker, M. R., Nesbitt, S. J., Kligman, B. T., Paluh, D. J., Marsh, A. D., Blackburn, D. C. & Parker, W. G. (2019): The earliest equatorial record of frogs from the Late Triassic of Arizona. – The Royal Society Publishing, **15**: 20180922.

Strömberg, C. A. E., Di Stilio, V. S. & Song, Z. (2016): Functions of phytoliths in vascular plants: an evolutionary perspective. – Functional Ecology, **30**: 1286–1297.

Sues, H.-D. (2003): An unusual new archosauromorph reptile from the Upper Triassic Wolfville Formation of Nova Scotia. – Canadian Journal of Earth Sciences, **40**: 635–649.

Sues, H.-D. & Olsen, P. E. (1993): A new procolophonid and a new tetrapod of uncertain, possibly procolophonian affinities from the Upper Triassic of Virginia. – Journal of Vertebrate Paleontology, **13**: 282–286.

Sues, H.-D. & Schoch, R. R. (2023): A new Middle Triassic (Ladinian) trilophosaurid stem-archosaur from Germany increases diversity and temporal range of this clade. – Royal Society Open Science, **10**: 230093.

Taborda, J. R. A., Desojo, J. B. & Dvorkin, E. N. (2021): Biomechanical skull study of the aetosaur *Neoaetosauroides engaeus* using finite element analysis. – Ameghiniana, **58**: 401–415.

Tseng, Z. J. (2012): Connecting Hunter-Schreger band microstructure to enamel microwear features: new insights from durophagous carnivores. – Acta Palaeontologica Polonica, **57**: 473–484.

Tucker, M. A. & Rogers, T. L. (2014): Examining predator–prey body size, trophic level and body mass across marine and terrestrial mammals. – Proceedings of the Royal Society, B: Biological Sciences, **281**: 20142103.

Ungar, P. S. (1994): Incisor microwear of Sumatran anthropoid primates. – American Journal of Physical Anthropology, **94**: 339–363.

Ungar, P. S. (2002): Microware software, version 4.02. A semi-automated image analysis system for the quantification of dental microwear. Fayetteville, AR, USA.

Ungar, P. S. (2015): Mammalian dental function and wear: A review. – Biosurface and Biotribology, **1**: 25–41.

Ungar, P. S., Teaford, M. F., Glander, K. E. & Pastor, R. F. (1995): Dust accumulation in the canopy: A potential cause of dental microwear in primates. – American Journal of Physical Anthropology, **97**: 93–99.

Varriale, F. J. (2016): Dental microwear reveals mammal-like chewing in the neoceratopsian dinosaur *Leptoceratops gracilis*. – PeerJ, **4**: e2132.

Walker, A., Hoeck, H. N. & Perez, L. (1978): Microwear of mammalian teeth as an indicator of diet. – Science, **201**: 908–910.

Werner, E. E. & Gilliam, J. F. (1984): The ontogenetic niche and species interactions in size-structured populations. – Annual Review of Ecology and Systematics, **15**: 393–425.

Williams, V. S., Barrett, P. M. & Purnell, M. A. (2009): Quantitative analysis of dental microwear in hadrosaurid dinosaurs, and the implications for hypotheses of jaw mechanics and feeding. – Proceedings of the National Academy of Sciences, **106**: 11194–11199.

Winkler, D. E., Schulz-Kornas, E., Kaiser, T. M. & Tütken, T. (2019): Dental microwear texture reflects dietary tendencies in extant Lepidosauria despite their limited use of oral food processing. – Proceedings of the Royal Society, B: Biological Sciences, **286**: 20190544.

Xafis, A., Saarinen, J., Bastl, K., Nagel, D. & Grímsson, F. (2020): Palaeodietary traits of large mammals from the middle Miocene of Gračanica (Bugojno Basin, Bosnia-Herzegovina). – Palaeobiodiversity and Palaeoenvironments, **100**: 457–477.

Young, M. T., Brusatte, S. L., Beatty, B. L., De Andrade, M. B. & Desojo, J. B. (2012): Tooth-on-tooth interlocking occlusion suggests macrophagy in the Mesozoic marine crocodylomorph *Dakosaurus*. – The Anatomical Record, **295**: 1147–1158.

Zanno, L. E. & Makovicky, P. J. (2011): Herbivorous ecomorphology and specialization patterns in theropod dinosaur evolution. – Proceedings of the National Academy of Sciences, **108**: 232–237.

Zuccotti, L. F., Williamson, M. D., Limp, W. F. & Ungar, P. S. (1998): Technical note: Modeling primate occlusal topography using geographic information systems technology. – American Journal of Physical Anthropology, **107**: 137–142.

Addresses of the authors:

Michael P. Mellett, Department of Biology, Virginia Tech, Blacksburg, VA 24061, USA; e-mail: michaelpm@vt.edu

Ben T. Kligman, Department of Geosciences, Virginia Tech, Blacksburg, VA 24061, USA & Petrified Forest National Park, 1 Park Road, Petrified Forest, AZ 86028, USA; e-mail: bkligman@vt.edu

Sterling J. Nesbitt, Department of Geosciences, Virginia Tech, Blacksburg, VA 24061, USA; e-mail: sjn2104@vt.edu

Michelle R. Stocker, Department of Geosciences, Virginia Tech, Blacksburg, VA 24061, USA; e-mail: stockerm@vt.edu

Manuscript received: 6 December 2022; revised version accepted 27 March 2023.

Table 1. Variation in dentition dimensions of two purportedly immature *Trilophosaurus buettneri* specimens. Height is dorsoventral, width is labiolingual, length is mesiodistal. Counting is from the most mesial tooth with a clear three-lophed form and skips empty sockets or other positions for which no measurements could be made. "?" denotes data that may exist but was not available to the authors. "X" denotes data not collectable (either because part of the element is missing or because it is not applicable). Digital measurements are from photos provided by M. Brown and W. Reyes.

Specimen	Source	Tooth position	Tooth height (mm)	Tooth width (mm)	Tooth length (mm)	Dentary height (mm)	Dentary width (mm)
SMU 77695	Direct Measurement	mesial	3.02	5.52	2.2	11.77	7.04
SMU 77695	Direct Measurement	distal	3.12	5.77	2.43	11.77	7.04
TMM 31099-15A (=26) (L)	Digitally measured	3	X	2.658	1.476	?	?
TMM 31099-15A (=26) (L)	Digitally measured	4	1.897	3.473	1.464	?	?
TMM 31099-15A (=26) (L)	Digitally measured	5	2.306	4.092	1.556	?	?
TMM 31099-15A (=26) (L)	Digitally measured	6	2.290	4.265	1.520	?	?
TMM 31099-15A (=26) (L)	Digitally measured	7	2.431	4.702	1.661	?	?
TMM 31099-15A (=26) (L)	Digitally measured	8	3.185	X	1.562	?	?
TMM 31099-15A (=26) (L)	Digitally measured	9	3.051	5.199	1.709	?	?
TMM 31099-15A (=26) (L)	Digitally measured	10	2.944	5.286	1.661	?	?
TMM 31099-15A (=26) (L)	Digitally measured	11	2.632	5.247	1.661	?	?
Mean			2.688	4.839	1.742	11.77	7.04

Table 2. Adult *Trilophosaurus buettneri* tooth and dentary measurements. Note that the identity of MNA V7064 is questionable given the significant stratigraphic gap between it and other *Trilophosaurus buettneri* specimens.

Specimen	Source	Tooth position	Tooth height (mm)	Tooth width (mm)	Tooth length (mm)	Dentary height (mm)	Dentary width (mm)
NMMNH P-34374	Digitally measured from (Spielmann et al. 2008, fig 9c, d)	isolated	0.88	2.46	0.85	x	x
Specimen from SMU 252	Digitally measured from (Spielmann et al. 2008, fig. 14)	isolated	2.60	6.57	2.05	x	x
NMMNH P-34373	Digitally measured from (Spielmann et al. 2008, fig. 9a, b)	isolated	1.42	3.33	1.38	x	x
MNA V7064	Digitally measured from (Spielmann et al. 2008, fig. 17)	isolated	1.06	x	0.67	x	x
NMMNH P-34291	Digitally measured from (Spielmann et al. 2008, fig. 8)	isolated	0.83	1.55	0.53	x	x
TMM 31025-143	Digitally measured from (Demar & Bolt 1981, fig. 5)	in jaw, unclear	3.68	8.68	2.76	?	?

Specimen	Source	Tooth position	Tooth height (mm)	Tooth width (mm)	Tooth length (mm)	Dentary height (mm)	Dentary width (mm)
TMM 31025-5(L)	Direct Measurement	2 (mesial)	x	5.68	2.40	24.32	14.29
TMM 31025-5(L)	Direct Measurement	3	3.04	7.22	2.11	24.32	14.29
TMM 31025-5(L)	Direct Measurement	4	3.08	8.37	2.60	24.32	14.29
TMM 31025-5(L)	Direct Measurement	5	4.00	8.90	2.85	24.32	14.29
TMM 31025-5(L)	Direct Measurement	6	3.33	8.94	2.84	24.32	14.29
TMM 31025-5(L)	Direct Measurement	7	3.33	9.78	3.21	24.32	14.29
TMM 31025-5(L)	Direct Measurement	8	3.15	10.11	2.75	24.32	14.29
TMM 31025-5(L)	Direct Measurement	9	3.48	10.85	3.45	24.32	14.29
TMM 31025-5(L)	Direct Measurement	10	3.27	11.35	3.32	24.32	14.29
TMM 31025-5(L)	Direct Measurement	11	3.54	11.64	3.30	24.32	14.29
TMM 31025-5(L)	Direct Measurement	12	2.57	9.02	2.68	24.32	14.29
TMM 31025-5(L)	Direct Measurement	13 (distal)	1.32	4.27	1.70	24.32	14.29
TMM 31025-142(R)	Direct Measurement	2 (mesial)	3.25	8.54	2.58	24.51	16.34
TMM 31025-142(R)	Direct Measurement	3	3.29	9.04	2.6	24.51	16.34
TMM 31025-142(R)	Direct Measurement	4	3.96	8.86	2.68	24.51	16.34
TMM 31025-142(R)	Direct Measurement	5	2.83	9.95	2.90	24.51	16.34
TMM 31025-142(R)	Direct Measurement	6	4.08	10.81	3.33	24.51	16.34
TMM 31025-142(R)	Direct Measurement	7	3.63	11.23	3.47	24.51	16.34
TMM 31025-142(R)	Direct Measurement	8	3.91	10.02	3.35	24.51	16.34
TMM 31025-142(R)	Direct Measurement	9	3.52	10.38	2.98	24.51	16.34
TMM 31025-142(R)	Direct Measurement	10	3.44	8.36	2.61	24.51	16.34
TMM 31025-142(R)	Direct Measurement	11 (distal)	2.30	3.69	1.66	24.51	16.34
TMM 31025-239(L)	Direct Measurement	3 (mesial)	2.60	5.42	2.02	x	x
TMM 31025-239(L)	Direct Measurement	4	x	6.51	2.59	x	x
TMM 31025-239(L)	Direct Measurement	5	3.34	8.28	2.65	x	x
TMM 31025-239(L)	Direct Measurement	6	3.23	8.90	2.86	x	x
TMM 31025-239(L)	Direct Measurement	7	3.41	9.51	2.62	x	x
TMM 31025-239(L)	Direct Measurement	8	3.84	10.14	3.16	x	x
TMM 31025-239(L)	Direct Measurement	9	3.94	10.05	3.04	x	x
TMM 31025-239(L)	Direct Measurement	10	3.70	9.37	2.85	x	x
TMM 31025-239(L)	Direct Measurement	11 (distal)	3.58	8.42	3.14	x	x
Mean			3.04	8.23	2.56	24.41	15.32

Table 3. SMU 77695 (*Trilophosaurus buettneri*) mean 2D dental microwear angle, standard deviation, pit, and scratch count data. Note that the angle is measured from the right (3 o'clock is zero degrees) and the angles have been adjusted as they were originally taken at a variety of angles in the SEM and were originally measured with the left at zero degrees. Also note the two labial images were taken from the mesial-most tooth while the others were taken from the distal-most tooth.

SEM image Number	Side of tooth	Adjusted Angle (degrees)	Angle Standard Deviation	Number of Pits	Number of Scratches	Pit-to-scratch Ratio
585	labial	111	32	208	660	0.315
587	labial	102	41	292	707	0.413
563	lingual	93	43	264	701	0.377
762	mesial	174	53	302	413	0.731
763	mesial	10	70	410	541	0.758
778	mesial	87	43	456	466	0.978
783	mesial	86	44	350	617	0.567
785	mesial	97	57	427	572	0.746
633	distal	25	50	175	806	0.217
634	distal	173	55	127	833	0.152
640	distal	145	70	318	464	0.685
643	distal	142	80	355	517	0.687
645	distal	154	44	444	555	0.800

Table 4. DMNH PAL 2018-05-0012 (*Trilophosaurus phasmalophos*) mean 2D dental microwear angle, standard deviation, pit, and scratch count data. All sites of analysis are on the ?mesial side.

SEM image Number	Adjusted Angle (degrees)	SD	Number of Pits	Number of Scratches	Pit-to-scratch Ratio
861	59	53	224	771	0.290
865	132	54	306	692	0.442
873	149	82	229	664	0.345
878	91	70	378	618	0.612
879	48	55	281	716	0.392
882	38	61	326	593	0.550
886	43	78	246	653	0.377
887	13	77	166	632	0.263

Table 5. PEFO 43837 dental pit and scratch count data. Note that sites of analysis are in occlusal view and the first letters of the image (e.g., T1) indicate which tooth it comes from with one being mesial-most and three being distal-most.

Image	Side	Number of Pits	Number of Scratches	Pit-to-Scratch Ratio
T1AP3	Occlusal	82	42	1.952
T1BP2	Occlusal	100	68	1.471
T1CP	Occlusal-distal	167	111	1.504
T2AP	Occlusal-labial	227	125	1.816
T2BP4	Occlusal	284	215	1.321
T3AP3	Occlusal-labial	356	119	2.992
T3BP4	Occlusal-mesial	157	91	1.725
T3CP	Occlusal-lingual	230	102	2.255

Table 6. PEFO 42082 (*Trilophosaurus phasmalophos*) dental pit and scratch count data. Note that enamel is missing in parts of all sites of analysis consistent with loss from taphonomic processes and/or preparation. Sites of analysis are in occlusal view with the labial side to the left and the lingual side to the right.

Image	Number of Pits	Number of Scratches	Pit-to-Scratch Ratio
A,PMT	224	535	0.419
A,PMT2	268	435	0.616
B,PLM3	48	114	0.421
B,PMT2	251	683	0.367

Table 7. Comparison of whole-tooth metrics between all specimens. Note that due to missing enamel, presence of debris, and non-perpendicular angle of imaging, sites of analysis from PEFO 42082 and PEFO 43837 have less reliable feature densities. SMU 77695* denotes data ignoring the mesial-most tooth. SMU 77695** denotes data ignoring the mesial-most tooth and the mesial side of the distal-most tooth. SD stands for standard deviation.

Specimen	Mean Feature Count	Feature Count SD	Mean Pit-to-Scratch Ratio	Pit-to-Scratch Ratio SD	Mean Feature Density per mm^2	Wear Feature Density SD
SMU 77695	921.538	89.111	0.526	0.252	14,969.753	1,447.547
SMU 77695*	936.777	70.363	0.540	0.283	15,207.313	1,142.998
SMU 77695**	926.500	83.284	0.434	0.273	15,050.357	1,352.899
DMNH PAL 2018-05-0012	936.875	72.890	0.404	0.121	15,218.892	1,184.051
PEFO 42082	639.500	333.191	0.448	0.110	11,197.689	5,834.200
PEFO 43837	309.500	133.534	1.836	0.539	54,193.661	2,3381.960